Bulk organic geochemistry of sediments from Puyehue Lake and its watershed (Chile, 40°S): Implications for paleoenvironmental reconstructions

Sébastien Bertrand[1,*], Mieke Sterken[2], Lourdes Vargas-Ramirez[3], Marc De Batist[4], Wim Vyverman[2], Gilles Lepoint[5], and Nathalie Fagel[6]

[1] Marine Chemistry and Geochemistry, Woods Hole Oceanographic Institution, 360 Woods Hole Road, MA02536, Woods Hole, USA. Tel: 1-508-289-3410, Fax: 1-508-457-2193

[2] Protistology and Aquatic Ecology, University of Ghent, Krijgslaan 281 S8, 9000 Gent, Belgium

[3] Instituto de Investigaciones Geológicas y del Medio Ambiente, Universidad Mayor de San Andrés, La Paz, Bolivia

[4] Renard Centre of Marine Geology, University of Ghent, Krijgslaan 281 S8, 9000 Gent, Belgium

[5] Oceanology Laboratory, University of Liège, 4000 Liège, Belgium

[6] Clays and Paleoclimate Research Unit, Sedimentary Geochemistry, University of Liège, 4000 Liège, Belgium

[*]Corresponding author: sbertrand@awi.de

Abstract (376 words)

Since the last deglaciation, the mid-latitudes of the southern Hemisphere have undergone considerable environmental changes. In order to better understand the response of continental ecosystems to paleoclimate changes in southern South America, we investigated the sedimentary record of Puyehue Lake, located in the western piedmont of the Andes in south-central Chile (40°S). We analyzed the elemental (C, N) and stable isotopic ($\delta^{13}C$, $\delta^{15}N$) composition of the sedimentary organic matter preserved in the lake and its watershed to estimate the relative changes in the sources of sedimentary organic carbon through space and time. The geochemical signature of the aquatic and terrestrial end-members was determined on samples of lake particulate organic matter (N/C: 0.130) and Holocene paleosols (N/C:

0.069), respectively. A simple mixing equation based on the N/C ratio of these end-members was then used to estimate the fraction of terrestrial carbon (f_T) preserved in the lake sediments. Our approach was validated using surface sediment samples, which show a strong relation between f_T and distance to the main rivers and to the shore. We further applied this equation to an 11.22 m long sediment core to reconstruct paleoenvironmental changes in Puyehue Lake and its watershed during the last 17.9 kyr. Our data provide evidence for a first warming pulse at 17.3 cal kyr BP, which triggered a rapid increase in lake diatom productivity, lagging the start of a similar increase in sea surface temperature (SST) off Chile by 1500 years. This delay is best explained by the presence of a large glacier in the lake watershed, which delayed the response time of the terrestrial proxies and limited the concomitant expansion of the vegetation in the lake watershed (low f_T). A second warming pulse at 12.8 cal kyr BP is inferred from an increase in lake productivity and a major expansion of the vegetation in the lake watershed, demonstrating that the Puyehue glacier had considerably retreated from the watershed. This second warming pulse is synchronous with a 2°C increase in SST off the coast of Chile, and its timing corresponds to the beginning of the Younger Dryas Chronozone. These results contribute to the mounting evidence that the climate in the mid-latitudes of the southern Hemisphere was warming during the Younger Dryas Chronozone, in agreement with the bipolar see-saw hypothesis.

Keywords: organic matter, lake sediments, carbon, nitrogen, Southern Hemisphere, deglaciation.

1. Introduction

The geochemistry of lake sedimentary organic matter generally provides important information that can be used to reconstruct paleoenvironmental changes in lakes and their

53 watersheds. Total organic carbon (TOC) is comprised of material derived from both
54 terrestrial and aquatic sources, and it is necessary to constrain these sources as well as
55 possible for improving the interpretation of paleoenvironmental and paleoclimate records. A
56 good understanding of the nature of the bulk sedimentary organic matter can also provide
57 clues to interpret age models based on radiocarbon measurement of bulk sediment samples
58 (Colman et al., 1996). It is now commonplace to assess the origin of lake sedimentary organic
59 matter using C/N ratios and carbon stable isotopes (e.g., Meyers and Teranes, 2001).
60 However, to accurately reconstruct the relative contribution of each of the sources, it is
61 essential to characterize these sources and look at the evolution of the geochemical properties
62 of the organic matter during transport and sedimentation. This is however rarely done in
63 paleoclimate and paleoenvironmental reconstructions.

64 Lake sedimentary organic matter is generally described as a binary mixture of terrestrial
65 and aquatic end members that can be distinguished by their geochemical properties. Aquatic
66 macrophytes generally have C/N atomic ratios between 4 and 10; whereas terrestrial plants,
67 which are cellulose-rich and protein-poor, produce organic matter that has C/N atomic ratios
68 higher than 20 (Meyers and Teranes, 2001). Similarly, the carbon ($\delta^{13}C$) and nitrogen ($\delta^{15}N$)
69 isotopic compositions of sedimentary organic matter have successfully been used to estimate
70 the content of terrestrial and aquatic sources (Lazerte, 1983). In freshwater environments,
71 however, the use of carbon and nitrogen stable isotopes is relatively limited because of the
72 similar isotopic values for both the terrestrial and aquatic organic sources. The carbon and
73 nitrogen isotopic composition of organic matter in lake sediments can however provide
74 important clues to assess past productivity rates and changes in the availability of nutrients in
75 surface waters (Meyers and Teranes, 2001).

76 One of the main questions in present-day paleoclimate research is the role of the
77 Southern Hemisphere in the initiation of abrupt and global climate changes during the Late

78 Quaternary. Several studies have demonstrated that climate records from Antarctic ice cores
79 are clearly asynchronous with the rapid changes of the Northern Hemisphere, and suggest that
80 abrupt paleoclimate changes are initiated in the Southern Hemisphere (Sowers and Bender,
81 1995; Blunier and Brook, 2001; EPICA Community Members, 2006).
82 Most of the paleoceanographic records available for the Southern Hemisphere follow a
83 similar pattern, with sea surface temperatures of the Southern Pacific increasing in phase with
84 Antarctic ice core records (Lamy et al., 2004, 2007; Kaiser et al., 2005; Stott et al., 2007).
85 What remains very controversial is the nature and timing of abrupt climate changes in the
86 mid-latitudes of the Southern Hemisphere, especially in terrestrial environments (Barrows et
87 al., 2007). In South America, currently available terrestrial records indicate either
88 interhemispheric synchrony (Lowell et al., 1995; Denton et al., 1999; Moreno et al., 2001),
89 asynchrony (Bennett et al., 2000; Ackert et al., 2008) or intermediate patterns (Hajdas et al.,
90 2003).
91 Here, we present an integrated bulk organic geochemical study of the Puyehue lake-
92 watershed system (Chile, 40ºS) to better understand the paleoenvironmental changes
93 associated with climate variability in the mid-latitudes of South America. We investigate the
94 bulk elemental and isotopic composition of the sedimentary organic matter deposited in the
95 lake and its watershed to determine the sources of sedimentary organic matter and estimate
96 their relative contribution through time. These data are then used to reconstruct
97 paleoenvironmental changes in South-Central Chile during the last 17.9 kyr.
98
99 **2. Location and setting**
100 Puyehue Lake (40°40'S, 72°28'W) is one of the large glacial, moraine-dammed
101 piedmont lakes that constitutes the Lake District in South-Central Chile (38–43°S; Campos et
102 al., 1989). It is located at the western foothill of the Cordillera de Los Andes (Fig. 1) at an

103 elevation of 185 m a.s.l.. The lake has a maximum length of 23 km, a maximum depth of 123
104 m and a mean depth of 76.3 m (Campos et al., 1989). It covers 165.4 km² and is characterized
105 by a complex bathymetry, with three sub-basins and a series of small bedrock islands in its
106 centre (Charlet et al., 2008, Fig. 1). The largest sub-basin occupies the western side of the
107 lake (WSB) and is almost completely isolated from the northern and eastern sub-basins by a
108 lake-crossing ridge, which is interpreted as the continuation of an onshore moraine (Bentley,
109 1997). The deepest sub-basin is located in the eastern side of the lake (ESB), although this
110 part of the lake receives large amounts of sediment through the Golgol and Lican rivers. The
111 northern sub-basin (NSB) is locked between the bathymetric ridge and the delta of Lican
112 River.

113 Puyehue Lake is oligotrophic and mainly P-limited (Campos et al., 1989). It has a high
114 transparency (mean Secchi depth: 10.7 m) and its high silica concentration (15 mg/l; Campos
115 et al., 1989) is characteristic of lakes located in volcanic environments. Phytoplankton
116 biomass is maximal in summer, with a pronounced dominance of Cyanobacteria (Campos et
117 al., 1989). Diatoms dominate the phytoplankton in late autumn, winter and early spring, when
118 the N and P levels are high (Campos et al., 1989). The bottom of the lake is oxic year-round
119 and the lake is stratified during the summer, with the depth of the thermocline varying
120 between 15 and 20 m (Campos et al., 1989).

121 The region of Puyehue has been shaped by a complex interaction between Quaternary
122 glaciations, volcanism, tectonics, and seismic activity. The lake is believed to occupy a glacial
123 valley over-deepened by Quaternary glacial advances (Laugenie, 1982) and is dammed to the
124 west by several moraine ridges (Bentley, 1997). Its catchment covers 1510 km² and extends
125 far to the east of the lake. It is surrounded by several active volcanoes (e.g., Puyehue-Cordon
126 de Caulle, Antillanca), which have a strong influence on the inorganic composition of the lake
127 and watershed sediments (Bertrand et al., 2008a; Bertrand and Fagel, 2008). The lake

128 catchment is essentially composed of Quaternary volcanic rocks covered by several metres of
129 post-glacial andosols, which frequently overly organic-poor glacial or fluvio-glacial deposits
130 (Bertrand and Fagel, 2008). The main tributaries to the lake are the Golgol River, which
131 drains more than 60 % of the lake watershed and the Lican River, which drains the western
132 part of the Puyehue-Cordon de Caulle volcanic complex (Fig 1). These two rivers are the
133 main sources of detrital input to the lake. They mainly supply particles to the eastern and
134 northern sub-basins. Of secondary importance are Chanleufu River and Pescadero River (Fig.
135 1). The lake is also fed from the north-west and south by a series of smaller rivers that
136 contribute relatively little to the detrital supply, because of the small size and relatively flat
137 morphology of their drainage basins (Fig. 1). For this reason, the detrital supply to the WSB is
138 very limited and the particles deposited in the WSB are primarily of autochthonous origin
139 (Bertrand et al., 2005). The outflow of Puyehue Lake (Pilmaiquen River) is located to the
140 west. It cross-cuts several moraine ridges (Laugenie, 1982; Bentley, 1997), merges with
141 Bueno River and flows westward into the Pacific.
142 The region of Puyehue has a humid temperate climate with Mediterranean influences. It
143 is linked to the global climate system via the southern Westerlies, which, combined with the
144 high relief of the Andes, are responsible for high precipitation in the area. Around the lake,
145 the annual rainfall averages 2000 mm/yr, and it increases with elevation up to 5000 mm/yr on
146 top of regional volcanoes (Parada, 1973; Muñoz, 1980). At Aguas Calientes, located in the
147 watershed of Puyehue Lake at ~ 5 km to the south-east of the lake, precipitation varies from
148 162 mm/month in summer to 524 mm/month in winter (Centro de Información Ambiental del
149 Parque Nacional de Puyehue, CONAF, pers. comm.; Fig. 1). Seasonality in rainfall is caused
150 by variations in the intensity and latitudinal position of the southern westerly wind belt, which
151 is presently centered at around 50°S in summer, and moves northward during winter. The
152 mean annual air temperature is 6 to 9°C, with maxima reaching 20°C in January and minima

of 2°C in July (Muñoz, 1980). Freezing sometimes occurs at night in winter, but a complete ice covering of the lake has never been observed (Thomasson, 1963). Snow cover occurs from May to November (Laugenie, 1982). This humid and temperate climate is responsible for the development of a dense temperate rainforest in the major part of the lake catchment (e.g., Moreno and Léon, 2003; Moreno, 2004).

3. Material and methods

3.1 Terrestrial and aquatic sources

In order to constrain the terrestrial sources of sedimentary organic matter deposited in Puyehue Lake, we conducted a sampling campaign in the watershed of the lake in January-February 2002. Samples of living vegetation (V), soils (SP), paleosols (OC) and river sediment (RS) were collected at representative locations of the lake watershed. Vegetation samples (V1 to V6) representing the six most abundant taxa were hand-picked from living plants and air dried on the field. The selection of these taxa was based on an extensive botanical study of the lake watershed (Vargas-Ramirez et al., 2008): *Podocarpus nubigena* (V1), Myrtaceae (V2), *Nothofagus dombeyi* (V3), Compositae (V4), Gramineae (V5) and *Trosterix corymbosus* (V6). Before analysis, the vegetation samples were oven dried at 40ºC for 48h, ground and homogenized using an agate mortar.

River sediment samples (RS) were collected at 21 locations selected in the main rivers flowing into Puyehue Lake (Fig. 1). Samples were collected using a trowel and avoiding coarse particles. The sediment samples were stored in air-tight Whirl-Pak plastic bags and freeze-dried in the laboratory.

Twelve paleosol samples were collected from 2 vertical profiles (outcrops) located at the southern (OC5) and northern (OC6) shores of the lake (Fig. 1). The outcrops are composed of fluvioglacial deposits overlain by several meters of brown silty loams, transformed into

178 andosols by weathering and pedogenetic processes (Bertrand and Fagel, 2008). The brown
179 silty loams are composed of volcanic ash deposited steadily during the Holocene and
180 therefore containing various levels of degraded organic matter.
181 In addition, we also collected 2 surface soil samples (SP) in the southern part of the lake
182 watershed, which is covered by the typical temperate rainforest. These samples contain
183 recently degraded organic matter and are therefore expected to be intermediate between the
184 OC and V types. The OC and SP samples were collected using a trowel and stored in air-tight
185 Whirl-Pak plastic bags. They were freeze-dried before preparation for analysis.
186 To constrain the aquatic source of sedimentary organic matter in Puyehue Lake, we
187 collected particulate organic matter (POM) at four stations across the lake (Fig. 1). Samples
188 were collected in summer (December) 2004, i.e. when productivity is the highest (Campos et
189 al., 1989), from the surface water in the Western (F2) and Eastern (F3 and F4) sub-basins, as
190 well as on top of the sublacustrine moraine ridge (PU-II site, F1). POM was collected on pre-
191 combusted fiberglass filters (Whatman GF/C) by filtering water samples until saturation.
192 Between 4.8 and 6.2 liters of lake water were filtered for each sample and the filters were air-
193 dried immediately after filtration. Samples were oven-dried at 40ºC for 24 hours before
194 analysis.
195
196 *3.2 Sedimentary organic matter*
197 In order to reconstruct temporal changes in the source and composition of sedimentary
198 organic matter, we sampled a 11.22 m long sediment core from the southern part of the lake.
199 The coring site (PU-II, 40º41.843' S, 72º25.341 W, Fig. 1) was selected after a preliminary
200 seismic investigation (Charlet et al., 2008). It is located on a plateau at a water depth of 48.4
201 m, and is ideally isolated from the direct influence of bottom currents (De Batist et al., 2008).
202 Coring operations were performed in February 2002 with a 3 m long Uwitec piston corer

operated from an anchored Uwitec platform. The sediment is composed of finely laminated to homogeneous brown silty particles (Bertrand et al., 2008a) and contains seventy-eight tephra layers, generally less than 1 cm thick and well distributed throughout the core (Bertrand et al., 2008b) (Fig. 2). Grain-size data have shown that the sediment of PU-II core contains 3 turbidites, at 379.5–381, 396.5–397.25 and 956–971 cm (Bertrand et al., 2008a).

The age model of core PU-II is based on 9 radiocarbon dates obtained on bulk sediment and 2 tephra layers related to historical eruptions (Fig. 2). The core covers the last 17.9 kyr and the radiocarbon dates are given in Table 1. Details concerning the age-model construction are given in Bertrand et al. (2008a). The radiocarbon age-model is consistent with accumulation rates calculated from ^{210}Pb and ^{137}Cs concentrations (Arnaud et al., 2006), as well as with the varve-counting data of Boës and Fagel (2008), and the tephrochronological model of Bertrand et al. (2008b).

In spring/summer 2002, the working half of the composite PU-II core was continuously sub-sampled in 1 cm thick slices. Samples were placed in plastic bags and stored at a constant temperature of 4ºC. For the present study, we selected samples every 10 cm from 0 to 750 cm, and every 5 cm below 750 cm. This represents a temporal sampling resolution of 60–300 years during the Holocene, and ~100 years during the last deglaciation. Samples were carefully selected avoiding sediment containing macroscopically visible tephra layers. Samples below tephra layers were preferred in order to discard a possible influence of tephras on vegetation and/or plankton, which may alter the sedimentary organic geochemical record. Before analysis samples were freeze-dried, ground and homogenized using an agate mortar. Finally, in order to test the validity of sedimentary organic matter geochemistry as a source proxy, we sampled surficial sediments at seven locations more or less influenced by direct detrital supply. Samples were taken in the 2 main sub-basins of the lake (ESB and WSB), as well as on the elevated platform located in the southern part of the lake. Samples were

228 collected using a short Uwitec gravity coring device (Bertrand et al., 2005). For the present
229 study, we selected the 0–1 cm samples only. These samples were freeze-dried and ground and
230 homogenized using an agate mortar.
231
232 *3.3. Sample preparation*
233 Before analysis, the freeze-dried samples from soils (SP), paleosols (OC), and river
234 sediment (RS) were sieved at 106 μm to discard particles coarser that those that reach the
235 lake. In order to estimate the organic content of the samples, three grams of sediment for each
236 terrestrial and lake sediment sample was separated for loss-on-ignition (LOI) measurements.
237 LOI was measured after 24h at 105°C (LOI_{105}), after an additional 4h at 550°C (LOI_{550}) and
238 after an additional 2h at 950°C to estimate water content, organic matter content and
239 inorganic carbonate content, respectively (Heiri et al., 2001). Because LOI_{550} is dependent on
240 the sample weight (Heiri et al. 2001), we always used 1g of dry samples (0.98 ± 0.09 g). For
241 the PU-II long core, we used the LOI_{550} data of Bertrand et al. (2008a). The LOI_{550} data were
242 used to optimize the weight of sediment used for carbon and nitrogen elemental and isotopic
243 analysis (between 15 and 75 mg for PU-II long core).
244
245 *3.4 Carbon and nitrogen elemental and isotopic analysis*
246 After freeze-drying and either grinding and homogenization in an agate mortar (lake
247 sediments) or sieving at 106 μm (SP, OC, RS), sediment samples were packed in tin
248 capsules, treated with 1N sulphurous acid to remove eventual carbonates (Verardo et al.,
249 1990) and analyzed at the UCDavis Stable Isotope Facility (USA). Total Organic Carbon
250 (TOC), Total Organic Nitrogen (TON) and stable isotope ratios of sedimentary carbon and
251 nitrogen were measured by continuous flow isotope ratio mass spectrometry (CF-IRMS;
252 20-20 SERCON mass spectrometer) after sample combustion to CO_2 and N_2 at 1000°C in

253 an on-line elemental analyzer (PDZEuropa ANCA-GSL). Before introduction to the
254 IRMS the gases were separated on a SUPELCO Carbosieve G column. Sample isotope
255 ratios were compared to those of pure cylinder gases injected directly into the IRMS before
256 and after the sample peaks and provisional $\delta^{15}N$ (AIR) and $\delta^{13}C$ (PDB) values were
257 calculated. Provisional isotope values were adjusted to bring the mean values of working
258 standard samples distributed at intervals in each analytical run to the correct values of the
259 working standards. The working standards are a mixture of ammonium sulfate and sucrose
260 with $\delta^{15}N$ vs Air = 1.33 ‰ and $\delta^{13}C$ vs PDB = -24.44 ‰. These standards are periodically
261 calibrated against international isotope standards (IAEA N1, N3; IAEA CH7, NBS22).
262 Total C and N are calculated from the integrated total beam energy of the sample in the
263 mass spectrometer compared to a calibration curve derived from standard samples of
264 known C and N content. The precision, calculated by replicate analysis of the internal
265 standard (mixture of ammonium sulfate and sucrose), is 0.09 ‰ for $\delta^{13}C$ and 0.14 ‰ for
266 $\delta^{15}N$.

267 For the POM (F1 to F4) and living vegetation (V1 to V6) samples, TOC, TON and $\delta^{13}C$
268 were measured on a FISONS NA 1500 NC elemental analyzer coupled with an Optima mass
269 spectrometer (VG IR-MS) at the Oceanology Laboratory, University of Liège, Belgium. For
270 $\delta^{13}C$ routine measurements are precise within 0.3 ‰. Vegetation samples were measured
271 twice (low and high mass) to optimize the signal for C and N, respectively.
272 Isotopic measurements are expressed relative to VPDB ($\delta^{13}C$) and AIR ($\delta^{15}N$) standards. For
273 C/N ratios, we always use the atomic C/N values (C/N weight ratio multiplied by 1.167), as
274 opposed to weight ratios, because they reflect the biogeochemical stoichiometry (Meyers and
275 Teranes, 2001). Carbonate has never been detected in our samples. Since our samples are
276 characterized by relatively high TOC, the residual inorganic nitrogen is negligible, and the

277 measured C/N ratios accurately reflect the organic matter sources (Meyers and Teranes,
278 2001).
279
280 **4. Results**
281 *4.1 Particulate organic matter*
282 The four lacustrine POM samples display C/N atomic ratios varying between 7.7 and
283 9.6 (8.5 ± 0.8) (average ± 1 σ; Table 2, Fig. 3). The highest value is observed for sample F3,
284 which is located near the mouth of the Golgol River, the main tributary and main source of
285 detrital particles to the lake (Fig. 1). The lowest value is associated with sample F2, collected
286 in the western sub-basin, and therefore protected from the direct influence of any river input.
287 The $\delta^{13}C$ values average -28.0 ‰ (± 2.0). The most negative value (-29.9 ‰) is associated to
288 sample F3. The $\delta^{15}N$ values vary between 0.7 and 3.6 ‰ (2.3 ± 1.5).
289
290 *4.2 Living vegetation*
291 The C/N atomic ratios of the six analyzed living vegetation samples are high and highly
292 variable (55.1 ± 21.8) (Fig. 3). The carbon isotopic values are less variable and they average -
293 29.7 ‰ (± 1.5). Interestingly, sample V5 (Gramineae) has the lowest atomic C/N ratio (28.1)
294 and the least negative $\delta^{13}C$ (-27.5 ‰). $\delta^{15}N$ has not been measured. These values are in the
295 range of values expected for terrestrial plants, and are in good agreement with the data
296 obtained by Sepúlveda (2005) on living vegetation samples from Northern Patagonia (C/N:
297 35.2 ± 13.6; $\delta^{13}C$: -30.3 ‰ ± 2.3). The wide range of C/N values found in fresh vegetation
298 represents the variety of species analyzed and reflects the natural variation in biochemical
299 composition of land plants (Meyers, 2003).
300
301 *4.3 Watershed sediment samples*

302 The C/N atomic ratio of the samples collected in the two paleosol profiles (OC) shows
303 an average of 14.6 (± 0.8). The two profiles are not significantly different from each other.
304 The only difference is the trend of C/N from the bottom to the top of the profiles, which is
305 increasing in OC5 and decreasing in OC6 (Fig. 4). Regarding the $\delta^{13}C$, the 2 outcrops are not
306 significantly different either, and the values average -25.7 ± 0.4 ‰. Both outcrops show a
307 slightly decreasing upward trend. The $\delta^{15}N$ values are highly variable and differ significantly
308 between OC5 (7.5 ± 0.7 ‰) and OC6 (6.0 ± 1.7 ‰).
309 The two soil samples (SP) show C/N atomic ratios of 15.5 and 23.1, and the isotopic
310 values are -25.5 ± 0.0 ‰ and 2.4 ± 4.5 ‰ for $\delta^{13}C$ and $\delta^{15}N$, respectively. The coarser than
311 106 um fraction has been analyzed separately and shows slightly different C/N ratios (17.6
312 and 21.8). The $\delta^{13}C$ values are not significantly different. Our C/N data are slightly lower than
313 the results obtained by Godoy et al. (2001) on soil samples from the Puyehue National Park
314 (atomic C/N: 24.5–25.5).
315 The C/N atomic ratio of the river sediment samples (RS14 to 34) averages 13.7 (± 1.1),
316 with the highest value for RS14 (15.6) and the lowest for RS24 (9.6). These values are not
317 clustered by river, nor correlated with the distance to/from the river mouth. It seems, however,
318 that samples collected in the southern part of the watershed have slightly higher C/N ratios.
319 The stable carbon isotopes display values ranging from -26.1 to -28.3 ‰ (-27.2 ± 0.5 ‰).
320 Samples with higher C/N ratios tend to have a more negative $\delta^{13}C$ ($r^2 = 0.53$). The $\delta^{15}N$
321 values average 2.0 (± 1.6) and show no correlation with either C/N or $\delta^{13}C$.
322
323 *4.4 Surface lake sediment samples*
324 The TOC of the surface lake sediment samples varies from 2.70 to 3.68 %. The average
325 C/N atomic ratio is 12.4 (± 1.7), with extreme values of 15.4 for PU-SC3 (southern shore) and

10.1 for PU-SC1 (western sub-basin) (Fig. 1). The surface sediment samples are characterized by a rather constant $\delta^{13}C$ of -28.0 ± 0.3 ‰, and by $\delta^{15}N$ of 0.7 ± 0.4 ‰.

4.5 Downcore record

The downcore record of TOC, C/N atomic ratios and $\delta^{13}C$ is illustrated in figure 2. The $\delta^{15}N$ data are not represented because they show no variation with depth (-0.3 ± 0.6 ‰). The TOC varies from 0.2 to 4.7 % (1.2 ± 0.7), with the lowest values being located under 830 cm (average: 0.5 %). The overall C/N trend is similar to that of TOC, with the lowest values occurring under 830 cm. The only exceptions to this trend are the extremely high (10.9 to 12.9) C/N atomic ratios within the turbidite layer at 956-971 cm. The presence of this turbidite also seems to affect the overlying values (between 956 to 935 cm), which are all very low (as low as to 2.9) and appear as "outliers" compared to the general trend. The $\delta^{13}C$ values vary between -25.0 and -28.5 ‰ (-27.4 ± 0.5 ‰), with the highest values occurring in the lower part of the core (Fig. 2), except for a more negative excursion between 870 and 1000 cm.

5. Discussion

5.1 Sources of sedimentary organic matter

The interpretation of organic geochemical records of lake sediments requires an accurate understanding of the sources of organic matter. In lake systems, organic matter is generally a mixture of aquatic and terrestrial end-members in varying proportions (Meyers and Teranes 2001). These two groups can generally be distinguished by their C/N ratio because lacustrine algae are characterized by C/N values ranging from 6 to 12, while vascular land plants create organic matter that usually has C/N ratios higher than 20 (Meyers and Teranes, 2001). Generally, stable carbon and nitrogen isotopes can also help identify the sources of

sedimentary organic matter (Lazerte, 1983). However, lake-derived organic matter that is produced by phytoplankton (C3 algae) using dissolved CO_2 is usually in equilibrium with the atmosphere and is therefore isotopically indistinguishable from organic matter produced by C3 plants in the surrounding watershed (Meyers and Teranes, 2001; Sifeddine et al., 2004). Therefore, carbon and nitrogen isotopes are generally of limited use to quantify organic matter sources in lake systems, but they can provide important information regarding the productivity rates and sources of nutrients.

5.1.1 Aquatic end-member

The stoichiometry of lake plankton is generally different from the Redfield ratio, as defined for marine plankton. The C/N ratio of lake plankton is generally around 10, but varies with nutrient availability and with species-specific characteristics (Sterner and Elser, 2002). One of the problems that arises in the determination of lake plankton stoichiometry is that samples, generally collected by filtration of lake water, may contain terrestrial particles. Although several studies provide evidence that the terrestrial contamination is negligible (Hecky et al., 1993), others attempt to correct for detrital contribution by regression analysis, assuming a constant element/chlorophyll ratio for lake organic matter. This correction is very approximate because it has been shown that the element/chlorophyll ratio varies largely with nutrient stress and light limitation (Healy and Hendzel, 1980). Therefore, correcting for detrital supply is generally not recommended, except for samples collected in small and shallow lakes, where detrital material is easily resuspended (Hecky et al., 1993); hence this approach has not been applied here.

The carbon stable isotopic values of lake plankton generally average -27‰ but vary significantly among species (Vuorio et al., 2006), with low values for chrysophytes and diatoms (-34.4 to -26.6 ‰) and high values for cyanobacteria (-32.4 ‰ to -5.9 ‰), which

dominate the plankton of Puyehue Lake (Campos et al., 1989). Similarly, the $\delta^{15}N$ values of lake plankton range from -2 to 13 ‰, with high values for chrysophytes, dinophytes and diatoms, and low values for cyanobacteria (Vuorio et al., 2006). In addition to inter-specific variability, carbon stable isotopes also vary with lake productivity. This relation is based on the observation that, during photosynthesis, phytoplankton preferentially consumes dissolved $^{12}CO_2$, which results in the production of ^{13}C-poor organic matter and removal of ^{12}C from surface water dissolved inorganic carbon (DIC). As the supplies of DIC become depleted, the $\delta^{13}C$ values of the remaining inorganic carbon increase and produce a subsequent increase in the $\delta^{13}C$ values of newly produced organic matter (Meyers and Teranes, 2001). Therefore, increased productivity yields an increase in $\delta^{13}C$ of organic matter that is produced in the lake and is available for sedimentation. $\delta^{15}N$ on the other hand, is essentially used to identify past changes in availability of nitrogen to aquatic producers (Talbot, 2001).

The four POM samples from Puyehue Lake were collected in summer, i.e. when precipitation is minimal. We therefore consider that the detrital influence is small and that our samples mostly represent the aquatic source of organic matter. Moreover, the samples were collected in the upper meter of the water column, which is only affected by virtually particle-free overflow currents.

The C/N atomic ratios of the 4 POM samples decrease with increasing distance to major river mouths. Samples collected in the eastern part of the lake probably contain a small fraction of terrestrial organic matter, as evidenced by their higher C/N ratios. The best example is sample F3 (C/N: 9.6) that is directly influenced by the supply of terrestrial particles through the Golgol River. This interpretation is supported by the low TOC value of this sample (19.6 %) compared to the other POM samples (Table 2). The sample collected in the western side of the lake (F2) is protected from any direct river input of terrestrial organic carbon, and is therefore used to determine the aquatic end-member (C/N: 7.7). This value is

close to the average C/N of the POM samples (8.5 ± 0.8) but better represents the purely autochthonous organic fraction. This relatively high value is in agreement with a low to moderate deficiency of Puyehue Lake in nitrogen, especially in summer when the productivity is high (Healey and Hendzel, 1980; Campos et al., 1989).

The $\delta^{13}C$ and $\delta^{15}N$ values average -28.0 and 2.3, respectively (Table 2), which is in agreement with the values observed for diatoms, and to a lesser extent, cyanobacteria in Finnish lakes (Vuorio et al., 2006). Interestingly, the most negative $\delta^{13}C$ value (-29.9) is associated to sample F3, which presumably contains a significant fraction of terrestrial organic matter. This might indicate that terrestrial carbon has low $\delta^{13}C$ values compared to the lake plankton.

5.1.2 Terrestrial end-member

Terrestrial organic matter originates from organisms living in the lake watershed. Before reaching lake systems, it generally gets exposed to various processes (e.g., degradation and remineralization by incorporation into soils, transportation by rivers etc) that alter its geochemical signature. In the literature, geochemical data obtained on living vegetation, soil, and river sediments samples have inconsistently been used to characterize the terrestrial end-member of sedimentary organic carbon (e.g., Colman et al., 1996; Baier et al., 2004; Sepúlveda, 2005), reflecting the difficulty of assigning a single geochemical value to the terrestrial end-member. Although Kendall et al. (2001) recognize that senescent leaves probably better represent the terrestrial end-member than fresh leaves, very few authors have looked at the geochemical transformations that occur during transport of organic matter from terrestrial environments to lake systems. In order to select the best terrestrial end-member for the sedimentary organic matter of Puyehue Lake, the geochemical composition of the possible sources of terrestrial sedimentary organic matter has been analyzed and is described hereunder.

426

427 a. Living vegetation

428 Terrestrial vegetation is characterized by C-rich, cellulose-rich and protein-poor
429 structural material, resulting in typically high C/N ratios, with reported averages of 36 ±
430 23 (Elser et al., 2000) or 43 (McGroddy et al., 2004) for foliage and 67 for litter
431 (McGroddy et al., 2004). Values as low as 7.5 and as high as 225 have been documented
432 (Sterner and Elser, 2002). Within a single large plant, leaves, stems and roots have highly
433 contrasting elemental composition, with leaves containing more nitrogen than any other
434 plant material (Sterner and Elser, 2002). Elemental variations are also linked to many
435 other variables, including growth conditions (nutrients, light, temperature, etc),
436 biogeography (latitude), and phylogenetic affiliation (Sterner and Elser, 2002). Some
437 authors argue that the stoichiometry of terrestrial plants can be grouped by biomes
438 (McGroddy et al., 2004). For temperate broadleaves, for example, values of 35 ± 4 for
439 foliage and 58 ± 4 for litter are to be expected (McGroddy et al., 2004). Therefore, a
440 single average C/N ratio does not accurately represent the natural vegetation of a complete
441 watershed.

442 The living vegetation samples collected in the watershed of Puyehue Lake show
443 typical C/N values of 55.1 ± 21.8, with large species-specific differences (Fig. 3).
444 Although some of the samples contained stems, most of our samples are composed of
445 leaves, as they represent the major fraction of organic matter reaching the lake.
446 The $\delta^{13}C$ of terrestrial vegetation is much more constant than its C/N ratio. It generally
447 averages -28 ‰, with extreme values of -25 and -29 ‰ for C3 plants (O'Leary, 1988) or -
448 23 to -31 ‰ (Meyers and Teranes, 2001). This relative constancy is due to the continuous
449 equilibrium exchange reactions that occur between vegetation and atmospheric CO_2.
450 Similarly, $\delta^{15}N$ of terrestrial vegetation generally varies between 2 and -6 (Fry, 1991).

451 The carbon isotopic composition of the 6 terrestrial taxa analyzed in the watershed of
452 Puyehue Lake ($\delta^{13}C$: -29.7 ± 1.5. Fig. 3) agrees with values generally accepted for
453 terrestrial vegetation, although on the low side. Our isotopic data are in perfect agreement
454 with data obtained on fresh vegetation samples from Northern Patagonia (-30.3 ± 2.3)
455 by Sepúlveda (2005).
456
457 b. Organic matter in soils and paleosols
458 Organic matter in soils originates from terrestrial organisms living at the surface of
459 soil profiles. It is in a constant state of decomposition (Post et al., 1985). The stable and
460 isotopic geochemical composition of soil organic matter consequently reflects the types of
461 plant that they host, minus the effect of biological degradation (Kendall et al., 2001). Even
462 after burial of the soil, soil organic matter (SOM) frequently decomposes further, resulting
463 in significant variations in its geochemical composition (Wynn, 2007). C/N ratios
464 typically decrease with depth (e.g., Boström et al., 2007; Nierop et al., 2007) due to the
465 microbial immobilization of nitrogenous material accompanied by the remineralization of
466 carbon (Meyers and Ishiwatari, 1993). Therefore, litter has a higher C/N ratio than the
467 humus derived from it, which has in turn a higher C/N ratio than the organic matter
468 incorporated in soil profiles (Post et al., 1985).
469 The $\delta^{13}C$ of SOM commonly increases with depth by 1 to 6 ‰ relative to the isotopic
470 composition of the original biomass (Boström et al., 2007; Wynn, 2007). The mechanisms
471 behind this process are still unclear but involve preferential decomposition of certain
472 components, variable mobility of sorption of dissolved organic carbon with variable
473 isotopic values, kinetic discrimination against ^{13}C during respiration and microbes as
474 precursors of stable organic matter (Boström et al., 2007). The $\delta^{15}N$ of soil organic matter
475 similarly increases up to 10‰ with depth (Nadelhoffer and Fry, 1988). Most of these

476 changes generally occur in the upper cm of soil profiles, resulting in a strong decrease of
477 C/N ratios and increase in $\delta^{13}C$ and $\delta^{15}N$ values in the first ~20 cm and stabilisation of
478 these values deeper in the profiles (Boström et al., 2007; Nierop et al., 2007).
479 In the two soil samples analyzed in the watershed of Puyehue Lake, the C/N of SOM
480 (19.3) is significantly lower than for living plants (55.1 ± 21.8). Similarly, we observe a
481 significant increase in $\delta^{13}C$ from -29.7 ‰ for terrestrial plants (V) to -25.6 ‰ for soil
482 organic matter (SP) (+ 4.1 ‰; Table 2). Compared to the soil samples (SP), the upper
483 paleosol samples (OC) show a significant decrease in C/N (from 19.3 to 14.6) but no
484 significant change in $\delta^{13}C$ (from -25.5 to -25.7 ± 0.4; Figs. 3, 4, Table 2). These relatively
485 high C/N values are typical for soils developed in humid and cold areas (Post et al., 1985,
486 Brady, 1990).
487 In the paleosol profile OC5, we observe a significant downward decrease in C/N, and
488 a slight increase in $\delta^{13}C$ and $\delta^{15}N$ (Fig. 4). The downward changes are less clear in profile
489 OC6 (Fig. 4). We observe globally constant C/N, $\delta^{13}C$ and $\delta^{15}N$ values, except for the
490 uppermost sample. In both profiles, the downward changes are lower than expected,
491 providing evidence that most of the geochemical changes occur during early soil burial.
492 The points representing the OC5 and OC6 samples are clearly grouped in the $\delta^{13}C$ versus
493 C/N diagram (Fig. 3), and are therefore easy to distinguish from other types of organic
494 matter. The only difference compared to the present-day soils is the decrease in C/N (Fig.
495 3). Compared to the living terrestrial vegetation, there is a clear decrease in both C/N and
496 $\delta^{13}C$ (Fig. 3).
497
498 c. River sediments
499 Although the organic matter transported by rivers is primarily of terrestrial origin
500 (Prahl et al., 1994), river plankton and macroorganisms can also contribute significantly to

501 the total budget (Kendall et al., 2001; Wissel et al., 2005). The terrestrial organic matter
502 transported by rivers is a mixture of relatively fresh organic matter from local vegetation
503 and organic matter previously incorporated in soils and paleosols, with their typical C/N
504 and $\delta^{13}C$ values (Fig. 3, Table 2). The C/N values of river plankton and microorganisms
505 are generally lower than 10 (Rostad et al., 1997; Kendall et al., 2001). Therefore, the C/N
506 composition of river POM and river sedimentary OM is generally between 8 and 15,
507 depending on the relative contribution of the autochthonous (river) and terrestrial sources,
508 respectively (Kendall et al., 2001). The difference in $\delta^{13}C$ between terrestrial and aquatic
509 (river) organic matter is generally not significant enough to discriminate between the two
510 sources of river organic matter (Kendall et al., 2001).
511 Our data show that the C/N values of the river sediment samples are slightly lower
512 than for the soils and paleosols (13.7 ± 1.1; Fig. 3). This is probably due to the combined
513 incorporation of (1) fresh vegetation, (2) degraded organic matter from soils and paleosols
514 and (3) river plankton. The low C/N ratios suggest a low contribution of fresh terrestrial
515 organic matter. In addition, the influence of river plankton on the C/N data seems
516 particularly important in Golgol River, where the 3 lowest C/N values have been
517 measured. This is in agreement with the relatively large size of this river, where the
518 aquatic productivity tends to contribute significantly to the total organic carbon content
519 (Vannote et al., 1980). If we assume that the river plankton has $\delta^{13}C$ values relatively
520 similar to the present-day vegetation (-29.7), the $\delta^{13}C$ values of the river sediment samples
521 (-27.2 ± 0.5) are also indicative of a mixture between river plankton and soils and
522 paleosols (-25.5 ± 0.0 and -25.7 ± 0.4, respectively).
523
524 *5.1.3 Selection of geochemical values for the aquatic and terrestrial end-members*

525 The data obtained on the watershed samples show a constant decrease of the C/N ratio
526 during degradation of terrestrial organic matter by incorporation into soils and transport to
527 Puyehue Lake (Fig. 3; Table 2). Although the river sediments represent most of the material
528 transported from the catchment to the lake, the geochemical values of these samples are also
529 affected by aquatic organic matter produced within the rivers, and can therefore not be used to
530 characterize the pure terrestrial end-member. Because the contribution of fresh vegetation to
531 the organic matter contained in river sediments seems relatively small, we argue that the
532 degraded organic matter contained in paleosols best represent the terrestrial end-member. The
533 C/N value used to define the terrestrial end-member is therefore 14.6 ± 0.8. Although the $\delta^{13}C$
534 values of the different sources of organic matter are not very distinct, we also use the $\delta^{13}C$ of
535 the paleosols (-25.7 ± 0.4 ‰) to characterize the terrestrial end-member. The $\delta^{15}N$ values of
536 the various sources of organic matter are too similar to define end-members and use them in
537 mixing equations.
538 For the aquatic end-member, we use the geochemical values of the sample of lake
539 particulate organic matter the least influenced by terrestrial detritus (F2, C/N: 7.7 and $\delta^{13}C$: -
540 28.2).
541 During the evaluation of the terrestrial and aquatic end-members we have shown that
542 living vegetation samples cannot be used to define the geochemical signature of the terrestrial
543 end-member. Studies that do so (e.g., Colman et al., 1996, Sepúlveda, 2005) don't take into
544 account the evolution of the geochemical properties of the organic matter during
545 incorporation into soils and transport by rivers. These papers therefore overestimate the
546 contribution of terrestrial organic matter to sedimentary environments.
547
548 *5.2 Mixing equation*

549 In the previous paragraph, we demonstrated that C/N ratios can be used to distinguish
550 between the aquatic and terrestrial sources of organic matter. These end-members can then be
551 used in a mixing equation to estimate the relative contribution of each source of organic
552 matter to lake sediments. Although figure 3 shows that the $\delta^{13}C$ data of Puyehue Lake
553 sediments roughly occur between the terrestrial and aquatic $\delta^{13}C$ values, the difference in $\delta^{13}C$
554 between the two end-members is too small to allow a precise quantification of the sources of
555 organic matter. Moreover, in lake systems, the $\delta^{13}C$ signature of sedimentary organic matter is
556 significantly driven by changes in productivity, altering the source organic matter signature.
557 Here, we use the C/N values of the aquatic and terrestrial end-members in a mixing equation
558 to estimate the proportion of terrestrially-derived organic carbon in the sediments of Puyehue
559 Lake. The use of such equations has recently been reviewed by Perdue and Koprivnjak
560 (2007), who demonstrate that mixing equations based on C/N data are always overestimating
561 the terrestrial fraction of organic carbon because C/N mixing lines are in reality curved.
562 Instead, the use of N/C in a simple linear mixing model (Eq. 1) permits the calculation of the
563 fraction of terrestrially derived carbon.

564 $$\frac{N}{C} = f_T\left(\frac{N}{C}\right)_T + f_A\left(\frac{N}{C}\right)_A \quad (1)$$

565 where f_T and f_A are the fractions of terrestrial and aquatic organic carbon, respectively. If we
566 assume that $f_T + f_A = 1$, we can then calculate the fraction of terrestrial organic carbon using
567 the following equation:

568 $$f_T = \frac{(N/C) - (N/C)_A}{(N/C)_T - (N/C)_A} \quad (2)$$

569 In addition to providing a linear relationship between the terrestrially derived organic
570 carbon and plankton-derived organic carbon (Perdue and Koprivnjak, 2007), using N/C ratios
571 has the advantage of providing similar ranges of variation for both the terrestrial (0.021 ±
572 0.008) and aquatic (0.118 ± 0.011) end-members and to simplify graphical representations

573 (Fig. 5). This equation can be applied to any sample of sedimentary organic matter from
574 Puyehue Lake, by using 0.130 for the aquatic end-member ($(N/C)_A$) and 0.069 for the
575 terrestrial end-member ($(N/C)_T$).
576
577 *5.3 Surface variability*
578 The proportion of terrestrial carbon contained in the 8 surface sediment samples has
579 been estimated from their bulk C/N data, using equation (2). The results show a clear relation
580 between the fraction of terrestrial carbon and the distance to the main lake tributaries and to
581 the shore (Fig. 6).The fraction of terrestrial carbon is the lowest (50 %) at site PU-SC1
582 (western sub-basin), which is protected from any direct river input (Fig. 1). It is the highest
583 (100 and 97%) at sites PU-SC3 and PU-SC7, respectively. These two sites are close to the
584 southern shore of the lake and probably receive direct inputs of terrestrial organic matter
585 during the rainy season (Figs. 1, 6). In addition, site PU-SC3 is directly influenced by the
586 plume of Pescadero River, which explains the very high fraction of terrestrial organic carbon
587 at this site (Fig. 1). The surface sample of site PU-II is intermediate (67%).
588
589 *5.4 Downcore variability*
590 Equation (2) was also applied to the C/N data of PU-II long core to estimate the
591 proportion of terrestrial carbon preserved in the sediments of Puyehue Lake since the end of
592 the Last Glacial Maximum. Although organic carbon concentrations generally decrease by a
593 factor of 10 during sinking and early diagenesis, the initial C/N and carbon isotopic ratios
594 remain relatively unchanged and can therefore be used to reconstruct past changes in organic
595 carbon sources (Meyers and Ishiwatari, 1993; Meyers, 2003).
596 Before interpreting any data in terms of paleoenvironmental and/or paleoclimate
597 changes, it is essential to carefully inspect the results and withdraw data associated to

598 instantaneously deposited sedimentary units (e.g., tephra layers, turbidites, etc). For PU-II
599 long core, samples were carefully selected to avoid the tephra layers, but some of the analyzed
600 samples were collected within a turbidite at 971-956 cm. These samples show anomalously
601 high C/N values (10–12), and the samples located immediately above the turbidite (956–935
602 cm) present extremely low C/N values (Fig. 2). The high C/N values between 971 and 956 cm
603 probably reflect the terrestrial origin of the sediment particles composing the turbidite. Above
604 the turbidite (956–935 cm), the low C/N values most likely reflect the increase in nutrients
605 (N, P) associated to the high supply of terrestrial material by the turbidite-triggering event.
606 Therefore, the geochemical data associated with the deposition of this turbidite have been
607 removed from the database used for paleoenvironmental and paleoclimate interpretations.
608 As shown in Figure 5, the N/C ratio of PU-II long core above 830 cm typically oscillates
609 between the aquatic and terrestrial end-members. Below 830 cm, however, the N/C values are
610 frequently higher than 0.130, reflecting the high nitrogen content of these samples. These high
611 N/C ratios cannot be explained by a simple mixing between the present-day aquatic and
612 terrestrial end-members, but are probably due to a combination of various factors, such as (1)
613 degradation of sedimentary organic matter during early diagenesis (loss of C), (2) high
614 nitrogen supply at the time of sedimentation, (3) different plankton communities below 830
615 cm (Sterken et al., 2008) characterized by different stoichiometries, or (4) seasonality of the
616 primary plankton communities: our POM samples were taken during summer and might
617 therefore contain less diatoms relative to Cyano- and Chlorophytes, which could make a
618 difference in the stoichiometry of the aquatic end-member (e.g., Arrigo, 2005). For these
619 samples, the application of equation (2) provides negative f_T values that were modelled to 0.
620 The resulting f_T plot is represented in figure 7. The fraction of terrestrial carbon
621 strikingly follows the total organic carbon ($r^2 = 0.72$, $p < 0.0001$), providing evidence that
622 most of the changes in TOC are due to changes in terrestrial organic matter. Before 12.8 cal

kyr BP the results show an extremely low fraction of terrestrial carbon, demonstrating that the main source of organic matter during the last deglaciation was aquatic. At 12.8 cal kyr BP, the TOC and f_T concomitantly increase, evidencing an increased supply in terrestrial organic matter, most likely linked to the development of the vegetation in the lake watershed. This increase seems to occur progressively between 12.8 and 11.2 cal kyr BP. After 11.2 cal kyr BP, the TOC and f_T remain generally high, with secondary decreases at 6.90–6.10 and 5.45–4.55 cal kyr BP. It is noteworthy that the $\delta^{13}C$ signal does not follow the changes in f_T, and therefore probably reflects changes in lake productivity instead of changes in the origin of the sedimentary organic matter. In addition, minor increases in $\delta^{13}C$ might be due to the development of C4 plants in the lake watershed, which was however relatively limited since plants using the C4 pathway are characteristic for dry and warm environments, such as tropical grasslands and savannah (Osborne and Beerling, 2006).

5.5 Implication for bulk radiocarbon ages

The important changes in the source of organic carbon through time have a direct influence on the interpretation of the bulk radiocarbon ages and on the construction of the age-depth model of PU-II long core. By using bulk samples for radiocarbon dating, Bertrand et al. (2008a) assumed that the radiocarbon ages represent the age of sediment deposition. However, since bulk samples contain a mixture of aquatic (syndepositional) and terrestrial (aged) organic matter, some of the ages might be older than the true age of deposition. As the two radiocarbon samples at 908 and 1012 cm (13,100–13,850 and 15,250–16,750 cal yr BP, respectively) do not contain any significant amount of terrestrial carbon (Fig. 7), they probably reflect a more correct age of deposition. For the samples younger than 12.8 cal yr BP, the fraction of terrestrial organic carbon is significant, making the bulk radiocarbon ages older than the age of sediment deposition since residence times of terrestrial organic matter in

lake watersheds is typically in the order of several hundred years (e.g., Drenzek et al., 2009). This interpretation is in agreement with the tephrochronological model of Bertrand et al. (2008b) who show that the radiocarbon dates of bulk samples encompassing the AD 1907 tephra are 500–600 years older than expected. Since these samples contain a significant amount (~60 %) of terrestrial carbon, we can assume that the terrestrial carbon reaching the lake is aged (~1000 years old), which justifies the use of the paleosol geochemical values to define the terrestrial end-member. Since the two lowermost radiocarbon dates are not affected by incorporation of old organic radiocarbon, the chronology of the lower part of the core (> 12.8 cal kyr BP) is accurate, which is crucial to discuss the changes associated with the deglaciation/Holocene transition.

5.6 Paleoenvironmental and paleoclimate interpretation and comparison with other proxies

In figure 7, the TOC and f_T data of PU-II long core are compared to sedimentological and paleoecological (pollen concentrations, diatom biovolumes) data previously obtained on the same sediment core (Bertrand et al., 2008a; Sterken et al., 2008; Vargas-Ramirez et al., 2008).

Sedimentological and diatom biovolume data show that the biogenic silica productivity of Puyehue Lake quickly increases at 17.3 ka (Fig. 7). This increase has been interpreted as the first warming pulse initiating the main phase of the deglaciation in South-Central Chile (Bertrand et al., 2008a; Sterken et al., 2008). The organic record of Puyehue Lake shows a small but significant concomitant increase in TOC, and only a minor shift in f_T. Most of the increase in TOC between 17.3–16.3 cal kyr BP is probably linked to the increased lake diatom productivity, as seen in the biogenic silica index and diatom biovolume records (Fig. 7). The minor increase in f_T that follows the warming pulse most likely reflects the very limited expansion of the vegetation cover in the lake watershed in response to the first

673 warming pulse, in agreement with palynological data (Vargas-Ramirez et al., 2008). At ODP
674 site 1233, which is located immediately off the coast of Chile at the same latitude as Puyehue
675 (Fig. 1), Lamy et al. (2007) demonstrated a gradual increase in sea surface temperature of
676 nearly 5°C between 18.8 and 16.7 cal kyr BP (Fig. 8). The comparison of the two records
677 shows a 1500 years delay in the increase of Puyehue Lake productivity compared to the start
678 of the SST increase (Fig. 8). This lagged response can be explained by the presence of a large
679 glacier in the watershed of Puyehue Lake, which delayed the increase in lake temperature,
680 decreased light availability through the influx of glacial melt water and clays, and largely
681 limited the expansion of the vegetation around the lake. The presence of such a glacier in the
682 watershed of Puyehue Lake is supported by geomorphological observations (Bentley, 1997),
683 and the observed response time seems typical for glaciers in the Chilean Andes (Hubbard,
684 1997; Lamy et al., 2004). The retreat of Andean glaciers after approx. 17.5 cal kyr BP is also
685 supported by geomorphological and palynological evidences from several sites between 40
686 and 42°S (Denton et al., 1999), and by the salinity record of ODP Site 1233, showing a strong
687 meltwater influence between ~17.8 and 15.8 cal kyr BP (Lamy et al., 2004).
688 The period between 17.3 and 12.8 cal kyr BP in the PU-II record is characterized by a
689 constantly low f_T, a moderately low TOC, and a decrease in the biogenic silica index, which
690 might indicate an increased replacement of diatoms by other types of aquatic organisms
691 (cyanobacteria, chlorophytes) during parts of the year. This relative decrease in biogenic silica
692 might have been caused by low nutrient supplies, low temperature, and/or reduced lake
693 mixing (Bertrand et al, 2008a; Sterken et al., 2008), resulting from a southward shift of the
694 Westerlies, as was deduced by a concomitant ice advance in the region of Magellan (Sudgen
695 et al., 2005). This model is supported by the $\delta^{13}C$ data, which show a depletion between 15.5
696 and 13.5 cal kyr BP, arguing for a decreased lake productivity. The low but significant pollen
697 concentration values during this period probably represent pollen grains originating from the

698 Coastal Cordillera and Central Depression and transported by the Westerlies, since the
699 fraction of terrestrial carbon originating from the lake watershed remains extremely low.
700 Interestingly, this period corresponds to nearly constant sea surface temperatures at site ODP
701 1233 (Lamy et al., 2007; Fig. 8). The presence of cold reversal during the deglaciation is not
702 clearly expressed in our organic geochemical data, but the low biogenic silica values observed
703 at around 13.2–12.7 cal kyr BP (Fig. 8) might reflect the presence of the Huelmo-Mascardi
704 cold reversal (*sensu* Hajdas et al., 2003), as argued by Bertrand et al. (2008a).
705 The period between 12.8 and 11.8 cal kyr BP corresponds to major changes in the core
706 and represents the transition from the last deglaciation to the Holocene (Figs. 7, 8). We
707 observe simultaneous increases in TOC, f_T, biogenic silica, and secondarily $\delta^{13}C$, most likely
708 reflecting a second major warming pulse. This important warming triggered an increase of
709 lake (mainly diatom) productivity and a subsequent rapid expansion and development of the
710 vegetation in the lake watershed (Fig. 7). The timing of this 2nd warming pulse in the sediment
711 of Puyehue Lake (12.8 cal kyr BP) falls into the first half of the Younger Dryas Chronozone
712 (Fig. 7) and therefore contributes to the mounting evidence that the mid-latitudes of the
713 Southern Hemisphere were warming during the Younger Dryas Chronozone, in agreement
714 with the bipolar see-saw hypothesis of Stocker (1998). These important changes in the
715 limnology of Puyehue Lake and in the vegetation cover in the catchment strikingly
716 correspond to a 2°C increase in the sea surface temperature of ODP site 1233 (Fig. 8). The
717 synchronicity of these abrupt changes in Puyehue and at ODP site 1233 probably demonstrate
718 that the glacier had nearly totally retreated from the lake watershed by that time and did not
719 delay the response of the different terrestrial proxies.
720 During the Holocene, the TOC and f_T data are generally high, especially between 11.2
721 cal kyr BP and 6.9 cal kyr BP. These high values at the beginning of the Holocene indicate a
722 luxuriant development of the terrestrial vegetation in the catchment area, most probably

723 indicating high temperatures (Moreno, 2004; Vargas-Ramirez et al., 2008). After 6.9 cal kyr
724 BP, we observe a slight overall decrease in lake productivity and in the density of the
725 vegetation cover, with several major decreases in terrestrial organic carbon at 6.90–6.10 and
726 5.45–4.55 cal kyr BP, as well as 4.10 and 3.25 cal kyr BP. These changes are not clearly
727 expressed in the other proxies (Fig. 7) but they might reflect periods of stronger volcanic
728 activity, affecting the terrestrial vegetation in the lake watershed (at 6.90–6.10 and 5.45–4.55
729 cal kyr BP) and the lake productivity (at 4.10 and 3.25 cal kyr BP). This interpretation is
730 supported by tephrochronological data, which suggest a high level of volcanic activity
731 between 7.0 and 5.5 cal kyr BP (Fig. 7; Bertrand et al., 2008b). In particular, three thick
732 tephra layers (55, 5, and 18 mm) occur between 6.9 and 6.8 cal kyr BP, and two others (13
733 and 5 mm) at 5500 cal yr BP, coeval with the onset of the low TOC and f_T values. The two
734 relatively less important decreases in TOC at 4.10 and 3.25 cal kyr BP are not reflected in the
735 f_T data but clearly stand out in the detrital vs biogenic index and diatom biovolume data.
736 These two minima occur immediately above two major tephra layers (20 and 22 mm thick)
737 that might have caused a decrease in lake productivity.
738
739 **6. Conclusions**
740 The bulk organic geochemistry of sediments from Puyehue Lake and its watershed
741 provides important information about the sources of sedimentary organic matter and changes
742 in their relative contribution through space and time. We demonstrated that the C/N ratio of
743 the potential sources of terrestrial organic matter in the lake watershed constantly decreases
744 during incorporation into soils and transport to sedimentary environments. Therefore, the
745 organic matter contained in paleosols best represents the terrestrial end-member. After careful
746 selection of the terrestrial and aquatic end-members, their N/C ratios were used in a simple
747 mixing equation to estimate the fraction of terrestrial carbon preserved in lake sediments. For

748 the recent sediments, we observe a direct relation between the fraction of terrestrial carbon
749 and the distance to the main tributaries and to the lake shore. In addition, we showed that
750 during the last 17.9 kyr, the TOC and the fraction of terrestrial carbon shift simultaneously
751 and reflect the expansion of the vegetation in the lake watershed. During the last deglaciation,
752 a first warming pulse at 17.3 cal kyr BP significantly increased the productivity of Puyehue
753 Lake, but the presence of a glacier in the lake watershed limited the concomitant expansion of
754 the terrestrial vegetation. Furthermore, the existence of the Puyehue glacier delayed the
755 response time of the terrestrial proxies by ~1500 years compared to the increase in sea surface
756 temperature. A second warming pulse is recorded in the sediments of Puyehue Lake at 12.8
757 cal kyr BP, and is synchronous with a 2°C increase in sea surface temperature, demonstrating
758 that the Puyehue glacier had significantly retreated from the lake watershed during the first
759 phase of the deglaciation. The timing of this second warming pulse corresponds to the
760 beginning of the Younger Dryas Chronozone, providing additional evidence for the absence
761 of a Younger Dryas cooling in southern South America. Finally, the Holocene is
762 characterized by an abundant vegetation cover probably linked to high temperatures between
763 11.2 and 6.9 cal kyr BP, and by several centennial-scale changes in lake plankton and
764 terrestrial vegetation, possibly caused by increased volcanic activity. These results add to the
765 mounting evidence that, during the last deglaciation, abrupt climate shifts in the Southern
766 Hemisphere led their Northern Hemisphere counterparts by at least 1000 years.
767
768 **Acknowledgments**
769 This research was partly supported by the Belgian OSTC project EV/12/10B "A
770 continuous Holocene record of ENSO variability in southern Chile". We acknowledge
771 François Charlet for the collection of the POM samples and Elie Verleyen for stimulating
772 discussions. Sediment cores were collected with the help of Fabien Arnaud, Christian Beck

(University of Savoie, France), Vincent Lignier (ENS Lyon, France), Xavier Boës (University of Liège, Belgium), Waldo San Martin, and Alejandro Peña (University of Concepción, Chile). The fieldwork in Chile has benefited from the logistic support of Roberto Urrutia (University of Concepción, Chile) and Mario Pino (University of Valdivia, Chile). S.B. is supported by a BAEF fellowship (Belgian American Educational Foundation), and by an EU Marie Curie Outgoing Fellowship under the FP6 programme.

780 **References**

781 Ackert, R., Becker, R., Singer, B., Kurz, M., Caffee, M., Mickelson, D., 2008. Patagonian
782 glacier response during the Late Glacial – Holocene transition. Science 321, 392–295.
783
784 Arnaud, F., Magand, O., Chapron, E., Bertrand, S., Boës, X., Charlet, F., Mélières, M.A.,
785 2006. Radionuclide profiles (^{210}Pb, ^{137}Cs, ^{241}Am) of recent lake sediments in highly active
786 geodynamic settings (Lakes Puyehue and Icalma – Chilean Lake District). Science of the
787 Total Environment 366, 837–850.
788
789 Arrigo, K., 2005. Marine microorganisms and global nutrient cycles. Nature 437, 349–355.
790
791 Baier, J., Lucke, A., Negendank, J.F.W., Schelser, G.-H., Zolitschka, B., 2004. Diatom and
792 geochemical evidence of mid- to late Holocene climatic changes at Lake Holzmaar, West-
793 Eifel (Germany). Quaternary International 133 (1), 81–96.
794
795 Barrows, T., Lehman, S.J., Fifield, L.K., De Deckker, P., 2007. Absence of Cooling in New
796 Zealand and the Adjacent Ocean During the Younger Dryas Chronozone. Science 318, 86–89.
797
798 Bennett, K.D., Haberle, S.G., Lumley, S.H., 2000. The last Glacial-Holocene transition in
799 southern Chile. Science 290, 325–328.
800
801 Bentley, M.J., 1997. Relative and radiocarbon chronology of two former glaciers in the
802 Chilean Lake District. Journal of Quaternary Science 12, 25–33.
803

804 Bertrand, S, Fagel, N., 2008. Nature, origin, transport and deposition of andosol parent
805 material in south-central Chile (36-42ºS). Catena 73 (1), 10–22.
806
807 Bertrand, S., Boës, X., Castiaux, J., Charlet, F., Urrutia, R., Espinoza, C., Charlier, B.,
808 Lepoint, G., Fagel, N., 2005. Temporal evolution of sediment supply in Lago Puyehue
809 (Southern Chile) during the last 600 years and its climatic significance. Quaternary Research
810 64, 163–175.
811
812 Bertrand, S., Charlet, F., Charlier, B., Renson, V., Fagel, N., 2008a. Climate variability of
813 Southern Chile since the Last Glacial Maximum: a continuous sedimentological record from
814 Lago Puyehue (40°S). Journal of Paleolimnology 39 (2), 179–195.
815
816 Bertrand, S., Castiaux, J., Juvigné, E., 2008b. Tephrostratigraphy of the Late Glacial and
817 Holocene sediments of Puyehue Lake (Southern Volcanic Zone, Chile, 40°S). Quaternary
818 Research 70, 343–357.
819
820 Blunier, T., Brook, E.J., 2001. Timing of millennial-scale climate change in Antarctica and
821 Greenland during the last glacial period. Science 291, 109–112.
822
823 Boës, X., Fagel, N., 2008. Relationships between southern Chilean varved lake sediments,
824 precipitation and ENSO for the last 600 years. Journal of Paleolimnology 39 (2), 237–252.
825
826 Boström, B., Comstedt, D., Ekblad, A., 2007. Isotope fractionation and 13C enrichment in
827 soil profiles during the decomposition of soil organic matter. Oecologia 153 (1), 89–98.
828

Brady, N.C., 1990. The nature and properties of soils (10th edition). MacMillan Publishing Company, NewYork.

Campos, H., Steffen, W., Agüero, G., Parra, O., Zúñiga, L., 1989. Estudios limnologicos en el Lago Puyehue (Chile): morfometria, factores fisicos y quimicos, plancton y productividad primaria. Medio Ambiente 10, 36–53.

Charlet, F., De Batist, M., Chapron, E., Bertrand, S., Pino, M., Urrutia, R., 2008. Seismic stratigraphy of Lago Puyehue (Chilean Lake District): new views on its deglacial and Holocene evolution. Journal of Paleolimnology 39 (2), 163–177.

Colman, S.M., Jones, G.A., Rubin, M., King, J.W., Peck J.A., Orem, W.H., 1996. AMS radiocarbon analyses from Lake Baikal, Siberia: challenges of dating sediments from a large, oligotrophic lake. Quaternary Science Reviews 15, 669–684.

De Batist, M., Fagel, N., Loutre, M.-F., Chapron, E., 2008. A 17,900-year multi-proxy lacustrine record of Lago Puyehue (Chilean Lake District): introduction. Journal of Paleolimnology 39 (2), 151–161.

Denton, G.H., Heusser, C.J., Lowell, T.V., Moreno, P.I., Andersen, B.G., Heusser, L.E., Schlüter, C., Marchant, D.R., 1999. Geomorphology, stratigraphy, and radiocarbon chronology of Llanquihue drift in the area of the southern lake district, seno reloncaví, and isla grande de Chiloé, Chile. Geografiska Annaler 81 A(2), 167–212.

853 Drenzek, N.J., Hughen, K.A., Montluçon, D.B., Southon, J.R., dos Santos, G.M., Druffel,
854 E.R.M., Giosan, L., Eglinton, T.I., 2009. A New Look at Old Carbon in Active Margin
855 Sediments. Geology, in press.
856
857 Elser, J.J., Fagan, W., Denno, R.F., Dobberfuhl, D.R., Folarin, A., Huberty, A., Interlandi, S.,
858 Kilham, S.S., McCauley, E., Schulz, K.L., Siemann, E.H., Sterner, R.W. 2000. Elemental
859 analysis illuminates nutritional constraints on terrestrial and freshwater food webs. Nature
860 408, 578–580.
861
862 EPICA Community Members, 2006. One-to-one coupling of glacial variability in Greenland
863 and Antarctica. Nature 444, 195–198.
864
865 Fry, B., 1991. Stable isotope diagrams of freshwater food webs. Ecology 72, 2293–2297.
866
867 Godoy, R., Oyarzún, C., Gerding, V., 2001. Precipitation chemistry in deciduous and
868 evergreen *Nothofagus* forest of southern Chile under a low- deposition climate. Basic and
869 Applied Ecology 2, 65–72.
870
871 Hajdas, I., Bonani, G., Moreno, P., Aritzegui, D., 2003. Precise radiocarbon dating of Late-
872 Glacial cooling in mid-latitude South America. Quaternary Research 59, 70–78.
873
874 Healey, F.P., Hendzel, L.L., 1980. Physiological indicators of nutrient deficiency in lake
875 phytoplankton. Canadian Journal of Fisheries and Aquatic Sciences 37, 442–453.
876

877 Hecky, R.E., Campbell, P., Hendzel, L.L., 1993. The stoichiometry of carbon, nitrogen, and
878 phosphorous in particulate matter of lakes and oceans. Limnology and Oceanography 38 (4),
879 709–724.
880
881 Heiri O., Lotter A.F., Lemcke G., 2001. Loss on ignition as a method for estimating organic
882 and carbonate content in sediments: reproducibility and comparability of results. Journal of
883 Paleolimnology 25, 101–110.
884
885 Hubbard, A., 1997. Modeling climate, topography and palaeo-glacier fluctuations in the
886 Chilean Andes, Earth Surface Processes and Landforms 22 (1), 79–92.
887
888 Kaiser, J., Lamy, F., Hebbeln, D., 2005. A 70-kyr sea surface temperature record off southern
889 Chile (Ocean Drilling Program Site 1233). Paleoceanography, 20.
890 doi:10.1029/2005PA001146
891
892 Kendall, C., Silva, S.R., Kelly, V.J., 2001. Carbon and nitrogen isotopic compositions of
893 particulate organic matter in four large river systems across the United States. Hydrological
894 Processes 15, 1301–1346.
895
896 Lamy, F., Kaiser, J., Ninnemann, U., Hebbeln, D., Arz, H.W., Stoner, J. 2004. Antarctic
897 timing of surface water changes off Chile and Patagonian ice sheet response. Science 304,
898 1959–1962.
899

900 Lamy, F., Kaiser, J., Arz, H.W., Hebbeln, D., Ninnemann, U., Timm, O., Timmermann, A.,
901 Toggweiler, J.R., 2007. Modulation of the bipolar seesaw in the Southeast Pacific during
902 Termination 1. Earth and Planetary Science Letters 259, 400–413.
903
904 Laugenie, C., 1982. La région des lacs, Chili méridional. Unpublished PhD thesis, Université
905 de Bordeaux III, 822 p.
906
907 Lazerte, B.D., 1983. Stable carbon isotope ratios: implications for the source of sediment
908 carbon and for phytoplankton carbon assimilation in Lake Memphremagog, Quebec.
909 Canadian Journal of Fisheries and Aquatic Sciences 40, 1658–1666.
910
911 Lowell, T. V., Heusser, C. J., Andersen, B.G., Moreno, P.I., Hauser, A., Heusser, L.E.
912 Schüchter, C., Marchant, D.R., Denton, G. H., 1995. Interhemispheric correlation of Late
913 Pleistocene Glacial events. Science 269, 1541–1549.
914
915 McGroddy, M.E., Daufresne, T., Hedin, L.O., 2004. Scaling of C:N:P stoichiometry in forests
916 worldwide: implications of terrestrial redfield-type ratios. Ecology 85**,** 2390–2401.
917
918 Meyers, P.A., 2003. Applications of organic geochemistry to paleolimnological
919 reconstructions: a summary of examples from the Laurentian Great Lakes. Organic
920 Geochemistry 34 (2), 261–289.
921
922 Meyers, P.A., Ishiwatari, R., 1993. Lacustrine organic geochemistry—an overview of
923 indicators of organic matter sources and diagenesis in lake sediments. Organic Geochemistry
924 20, 867–900.

Meyers, P.A., Teranes, J.L., 2001. Sediment Organic Matter. In: Last, W.M., Smol, J.P. (Eds), Tracking environmental changes using lake sediment - Vol. 2: Physical and geochemical methods. Kluwer Academic, Dordrecht, The Netherlands, pp. 239–270.

Moreno, P.I., 2004. Millenial-scale climate variability in northwest Patagonia over the last 15000 yr. Journal of Quaternary Science 19, 35–47.

Moreno, P.I., Leon, A.L., 2003. Abrupt vegetation changes during the last glacial to Holocene transition in mid-latitude South America. Journal of Quaternary Science 18, 1–14.

Moreno, P.I., Jacobson, G.L.J., Lowell, T.V., Denton, G.H. 2001. Interhemispheric climate links revealed by a late-glacial cooling episode in southern Chile. Nature 409, 804–808.

Muñoz, M., 1980. Flora del parque nacional Puyehue. Universitaria, Santiago, 557 p.

Nadelhoffer, K.J., Fry, B., 1988. Controls on natural nitrogen-15 and carbon-13 abundances in forest soil organic matter. Soil Science Society of America Journal 52, 1633–1640.

Nierop, K.G.J., Tonneijck, F.H., Jansen, B., Verstraten, J.M., 2007. Organic matter in volcanic ash soils under forest and Páramo along an Ecuadorian altitudinal transect. Soil Science Society of America Journal 71, 1119–1127.

O'Leary, M.H., 1988. Carbon isotopes in photosynthesis. Bioscience 38, 328–336.

950 Osborne, C.P., Beerling, D.J., 2006. Nature's green revolution: the remarkable evolutionary
951 rise of C4 plants. Philosophical Transactions of the Royal Society, Series B 361, 173–194.
952
953 Parada, M.G. 1973. Pluviometria de Chile. Isoyetas de Valdivia-Puerto Montt. CORFO
954 Departamento de Recursos hydraulicos, 73 p.
955
956 Perdue, E.M., Koprivnjak, J.-F., 2007. Using the C/N ratio to estimate terrigenous inputs of
957 organic matter to aquatic environments. Estuarine Coastal and Shelf Science 73 (1–2), 65–72.
958
959 Post, W.M., Pastor, J., Zinke, P.J., Stangenberger, A.G., 1985. Global patterns of soil nitrogen
960 storage. Nature 317, 613–616.
961
962 Prahl, F.G., Ertel, J.R., Goni, M.A., Sparrow, M.A., Eversmeyer, B., 1994. Terrestrial organic
963 carbon contributions to sediments on the Washington margin. Geochimica Cosmochimcia
964 Acta 58, 3035–3048.
965
966 Rostad, C.E., Leenheer, J.A., Daniel, S.R., 1997. Organic carbon and nitrogen content
967 associated with colloids and suspended particulates from the Mississippi River and some of
968 its tributaries. Environmental Science and Technology 31, 3218–3225.
969
970 Schiefer, E., 2006. Contemporary sedimentation rates and depositional structures in a
971 Montane Lake, Coast Mountains, British Columbia, Canada. Earth Surface Processes and
972 Landforms 31, 1311–1324.
973

974 Sepúlveda, J., 2005. Aporte de material terrigeno en fiordos de Patagonia del Norte:
975 Evidencia geoquimica en sedimentos recientes y del Holoceno tardio. University of
976 Concepción, Chile. Unpublished Master thesis.
977
978 Sifeddine, A., Wirrmann, D., Luiza A., Albuquerque, S., Turcq, B., Campello Cordeiro, R.,
979 H.C. Gurgel, M., Joao Abrao, J., 2004. Bulk composition of sedimentary organic matter used
980 in palaeoenvironmental reconstructions: examples from the tropical belt of South America
981 and Africa. Palaeogeography, Palaeoclimatology, Palaeoecology 214 (1-2), 41–53.
982
983 Sowers, T. A., Bender, M., 1995. Climate records during the last deglaciation. Science 269,
984 210–214.
985
986 Sterken, M., Verleyen, E., Sabbe, K., Terryn, G., Charlet, F., Bertrand, S**.**, Boës, X., Fagel,
987 X., De Batist, M., Vyverman, W., 2008. Late Quaternary climatic changes in Southern Chile,
988 as recorded in a diatom sequence of Lago Puyehue (40°40'S). Journal of Paleolimnology 39
989 (2), 219–235.
990
991 Sterner R.W., Elser J.J., 2002. Ecological Stoichiometry: the Biology of Elements from
992 Molecules to the Biosphere. Princeton University Press, Princeton.
993
994 Stocker, T.F., 1998. The seesaw effect. Science 282**,** 61–62.
995
996 Stott, L., Timmermann, A, Thunell, R., 2007. Southern Hemisphere and Deep Sea Warming
997 led deglacial Atmospheric CO2 rise and Tropical Warming. Science 318, 435–438.
998

999 Sudgen, E., Bentley, M.J., Fogwill, C.J., Hulton, N.R.J., McCulloch, R.D., Purves, R.S.,
1000 2005. Late-glacial glacier events in southernmost south America: A blend of 'Northern' and
1001 'Southern' hemispheric climatic signals? Geografiska Annaler, Series A: Physical Geography
1002 87 (2), 273–288
1003
1004 Talbot, M. R. 2001. Nitrogen isotopes in palaeolimnology. In: Last, W. M., Smol, J.P. (Eds.),
1005 Tracking Environmental Change Using Lake Sediments. Volume 2: Physical and
1006 Geochemical Techniques. Kluwer Academic Publishers, Dordrecht, The Netherlands, pp.
1007 401–439
1008
1009 Thomasson K., 1963. Araucanian Lakes. Acta Phytogeographica Sueca 47, 1–139.
1010 Vannote, R.L., Minshall, G.W., Cummins, K.W., Sedell, J.R., Cushing, C.E., 1980. The river
1011 continuum concept. Canadian Journal of Fisheries and Aquatic Sciences 37, 130–137.
1012
1013 Vargas-Ramirez, L., Roche, E., Gerrienne, P., Hooghiemstra, H., 2008. A pollen-based record
1014 of late glacial–Holocene climatic variability in the southern lake district, Chile. Journal of
1015 Paleolimnology, 39 (2), 197–217.
1016
1017 Verardo, D.J., Froelich, P.N., McIntyre, A., 1990. Determination of organic carbon and
1018 nitrogen in sediments using the Carlo-Erba NA-1500 analyzer. Deep-Sea Research 37, 157–
1019 165.
1020
1021 Vuorio, K., Meili, M., Sarvala, J., 2006. Taxon-specific variation in the stable isotopic
1022 signatures ($\delta^{13}C$ and $\delta^{15}N$) of lake phytoplankton. Freshwater Biology 51, 807–822.
1023

1024 Wissel, B., Gace, A., Fry, B., 2005. Tracing river influences on phytoplankton dynamics in
1025 two Louisiana estuaries. Ecology 86, 2751–2762.
1026
1027 Wynn, J.G., 2007. Carbon isotope fractionation during decomposition of organic matter in
1028 soils and paleosols: Implications for paleoecological interpretations of paleosols,
1029 Palaeogeography, Palaeoclimatology, Palaeoecology 251 (3-4), 437–448.

Figure captions

Fig. 1 – Location of Puyehue Lake in South-Central Chile. The position of the coring sites is located on the bathymetric map of Campos et al., 1989. WSB, NSB, and ESB refer to the western, northern and eastern sub-basins of the lake, as described by Charlet et al. (2008). The position of river samples RS14 and RS24 is indicated, as these two samples have the highest (15.6) and lowest (9.6) C/N values, respectively.

Fig. 2 – Bulk organic geochemical data obtained on sediment core PU-II. Note the presence of a turbidite at 956–971 cm. The lithology and age-model are represented according to Bertrand et al. (2008a). The AMS radiocarbon results are given in Table 1.

Fig. 3 – C/N vs $\delta^{13}C$ biplots of the aquatic, terrestrial and sediment samples. The vegetation samples represent the most common regional species (1: Podocarpus Nubigena; 2: Myrtaceae; 3: Nothofagus Dombeyii; 4: Compositae; 5: Gramineae; 6: Trosterix corymbosus). For PU-II long core, the data from 971 to 935 cm were not included because of their association with a major turbidite (see figure 4). For colour figure, the reader is referred to the online version of this article.

Fig. 4 – Bulk organic geochemical data (TOC, atomic C/N, $\delta^{13}C$, $\delta^{15}N$) obtained on two paleosol outcrops occurring at the southern (OC5) and northern (OC6) shores of Puyehue Lake. For location, see figure 1. The profiles are essentially composed of volcanic ash deposited continuously during the Holocene (Bertrand and Fagel, 2008). The base of the outcrops (< 0 m) is believed to date from the last deglaciation, from geomorphological, tephrostratigraphical and mineralogical evidences (Bertrand and Fagel, 2008).

Fig. 5 – N/C vs $\delta^{13}C$ biplot of terrestrial, aquatic and lake sediment samples. The N/C average and standard deviation (1σ) of the main groups of samples are also shown. The downcore evolution of the N/C ratio is represented, with indication of the N/C values selected for the terrestrial (0.069) and aquatic (0.130) end-members. A comparison with figure 2 clearly shows the adequacy of using N/C instead of C/N for graphical representation of aquatic, terrestrial and sedimentary data. For PU-II long core, the samples located within and immediately above the turbidite are shown by the dark and light grey shaded areas, respectively. For colour figure, the reader is referred to the online version of this article.

Fig. 6 – Relation between the fraction of terrestrial carbon contained in the surface sediment samples of Puyehue Lake and the distance to river and shore index, calculated as Log (distance to main river) + 0.5 Log (distance to secondary river) + 0.5 Log (distance to shore). The main (bigger) rivers are Rio Golgol and Rio Lican, and the secondary rivers are Rio Pescadero and Rio Chanleufu. Distances to secondary river and shore were given half weighting to account for their smaller contribution to the total sediment supply compared to major rivers. We used the logarithm of the distance to account for the globally exponential decrease of sediment accumulation rate with increasing distance to the source (Schiefer, 2006). Local variations might be explained by differences in basin shape and height of the water column.

Fig. 7 – Comparison of geochemical, paleoecological and sedimentological data obtained on PU-II long core. The results are plotted versus time, according to the age-depth model of Bertrand et al. (2008a). The fraction of terrestrial carbon (f_T) is calculated using the N/C mixing equation (equation 2), with N/C values of 0.130 for the aquatic end-member and 0.069 for the terrestrial end-member. See text for details. Negative values (mainly below 830 cm)

have been set to zero. The data from 971 to 935 cm were not included because of their association with a major turbidite. The aquatic organic carbon data ($_{aq}$OC) were calculated as TOC * (1 - f_T). The biogenic silica index is used to indicate the relative importance of diatoms in the total aquatic community (dimensionless). The pollen concentration data are from Vargas-Ramirez et al. (2008). Two data points (159–160 cm and 179–180 cm) have been removed from the original database because of the presence of a tephra layer in these samples, leading to extremely low pollen concentrations. The detrital *vs* biogenic index is issued from Bertrand et al. (2008a). Positive values indicate high terrestrial content (driven by the sediment content in Ti, Al and magnetic susceptibility), and low values indicate a high biogenic content of the sediment (driven by biogenic silica, LOI_{550}, LOI_{105}, and grain-size, which is in turn directly related to the diatom content of the sediment). The diatom biovolume data are from Sterken et al. (2008). In addition, the tephra thickness of the most important tephras (≥ 10 mm thick) is represented according to Bertrand et al. (2008b). The TOC, aqOC, f_T, $\delta^{13}C$, biogenic silica index and detrital *vs* biogenic index data are represented as 3 points running averages. The original pollen concentrations and diatom biovolumes data have a lower temporal resolution (20 cm) and have therefore not been smoothed.

Fig. 8 – Sea surface temperature of ODP Site 1233 compared to two paleoenvironmental records from Puyehue Lake. (A) Alkenone sea-surface temperature from ODP site 1233 (Lamy et al., 2007); (B) Biogenic silica content of sediment core PU-II (Bertrand et al., 2008a); (C) Fraction of terrestrial carbon in sediment core PU-II (this study).

Table captions

Table 1 – AMS radiocarbon dates obtained on bulk sediment samples of PU-II long core. Calendar ages have been calculated using the Intcal98 calibration curve. For more details regarding the radiocarbon dates and age-model, see Bertrand et al. (2008a).

Table 2 – Average and standard deviation (± 1σ) of the bulk organic geochemical data obtained on Puyehue Lake and watershed sediment samples. The values obtained on the lake particulate organic matter (POM) and living vegetation are also indicated. n refers to the number of analyzed samples. [a] not measured on F3, [b] also includes PU-I-P5 and PU-II-P5, [c] from Bertrand et al. (2005).

Depth (mblf)	Laboratory n°	^{14}C age ± 1σ (yr BP)	2σ error range calibrated ages (OxCal) (cal yr BP)	Weighted Average (BCal) (cal yr BP)
120.5 cm	Poz-5922	2570 ± 35	2490 - 2770 (95.4 %)	2655
156.5 cm	Poz-1406	2590 ± 40	2490 - 2790 (95.4 %)	2681
306.5 cm	Poz-7660	4110 ± 40	4510 - 4830 (92.7 %)	4648
400.5 cm	Poz-2201	5300 ± 40	5940 - 6200 (95.4 %)	6074
463.75 cm	Poz-5923	5760 ± 40	6440 - 6670 (95.4 %)	6560
627.75 cm	Poz-5925	7450 ± 50	8160 - 8390 (93.9 %)	8262
762 cm	Poz-1405	10,010 ± 60	11,200 – 11,750 (91.0 %)	11,494
908 cm	Poz-7661	11,440 ± 80	13,100 – 13,850 (95.4 %)	13,407
1012 cm	Poz-2215	13,410 ± 100	15,250 – 16,750 (95.4 %)	16,063

Bertrand et al – Table 1

1113

Sample type	n	TOC (%)	C/N	N/C	$\delta^{13}C$ (‰)	$\delta^{15}N$ (‰)
Living vegetation (V1-6)	6	46.0 ± 3.6	55.1 ± 21.8	0.021 ± 0.008	-29.7 ± 1.5	--
Particulate organic matter (F1-4)	4	28.5 ± 7.6	8.5 ± 0.8	0.118 ± 0.011	-28.0 ± 2.0	2.3 ± 1.5[a]
Paleosols (OC5-6)	12	4.0 ± 1.6	14.6 ± 0.8	0.069 ± 0.004	-25.7 ± 0.4	6.8 ± 1.5
Present-day soils (SP2-3)	2	3.3 ± 3.6	19.3 ± 5.4	0.054 ± 0.015	-25.5 ± 0.0	2.4 ± 4.5
River sediment (RS14-34)	21	3.4 ± 2.3	13.7 ± 1.1	0.073 ± 0.006	-27.2 ± 0.5	2.0 ± 1.6
Surface sediment samples (SC1-7)[b]	8	3.2 ± 0.4	12.4 ± 1.7	0.082 ± 0.011	-28.0 ± 0.3	0.7 ± 0.4
PU-II short core (0-53 cm)[c]	53	2.5 ± 0.6	11.1 ± 0.7	0.091 ± 0.006	-28.1 ± 0.4	--
PU-II long core (0-1122 cm)	146	1.2 ± 0.7	9.0 ± 1.8	0.117 ± 0.036	-27.4 ± 0.5	-0.3 ± 0.6

1114

1115 Bertrand et al – Table 2

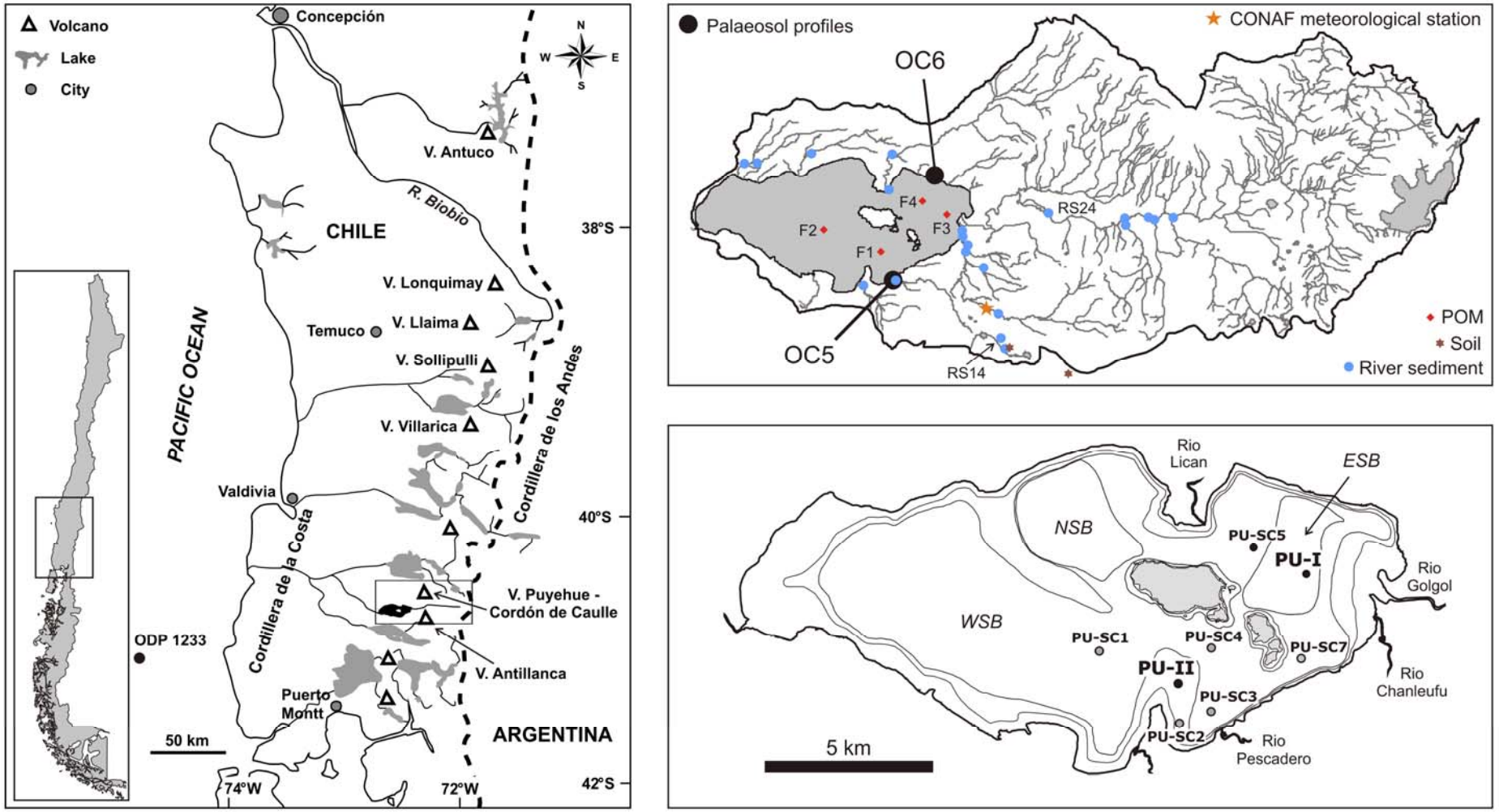

Bertrand et al – Figure 1

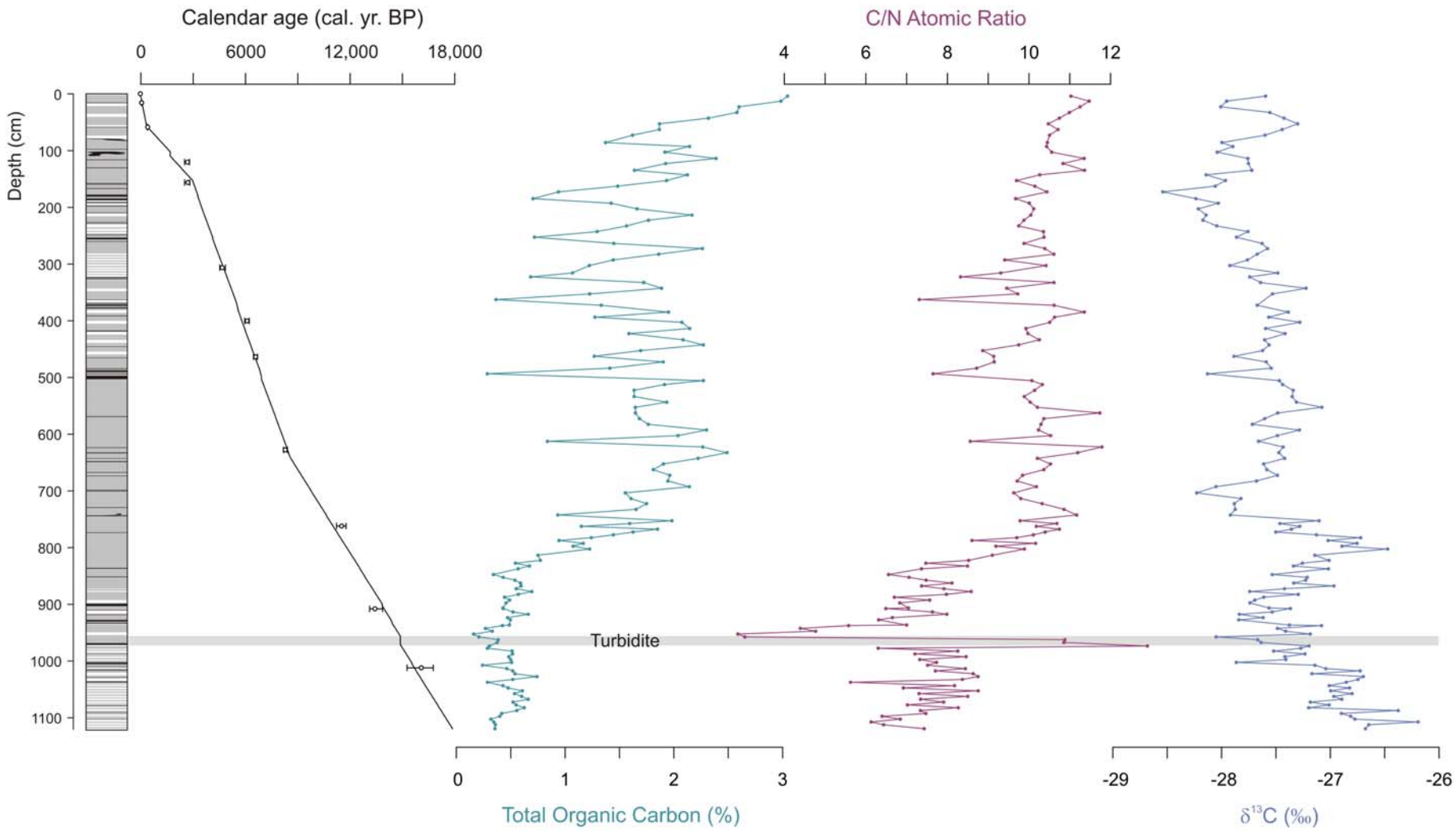

1118

1119 Bertrand et al – Figure 2

1120

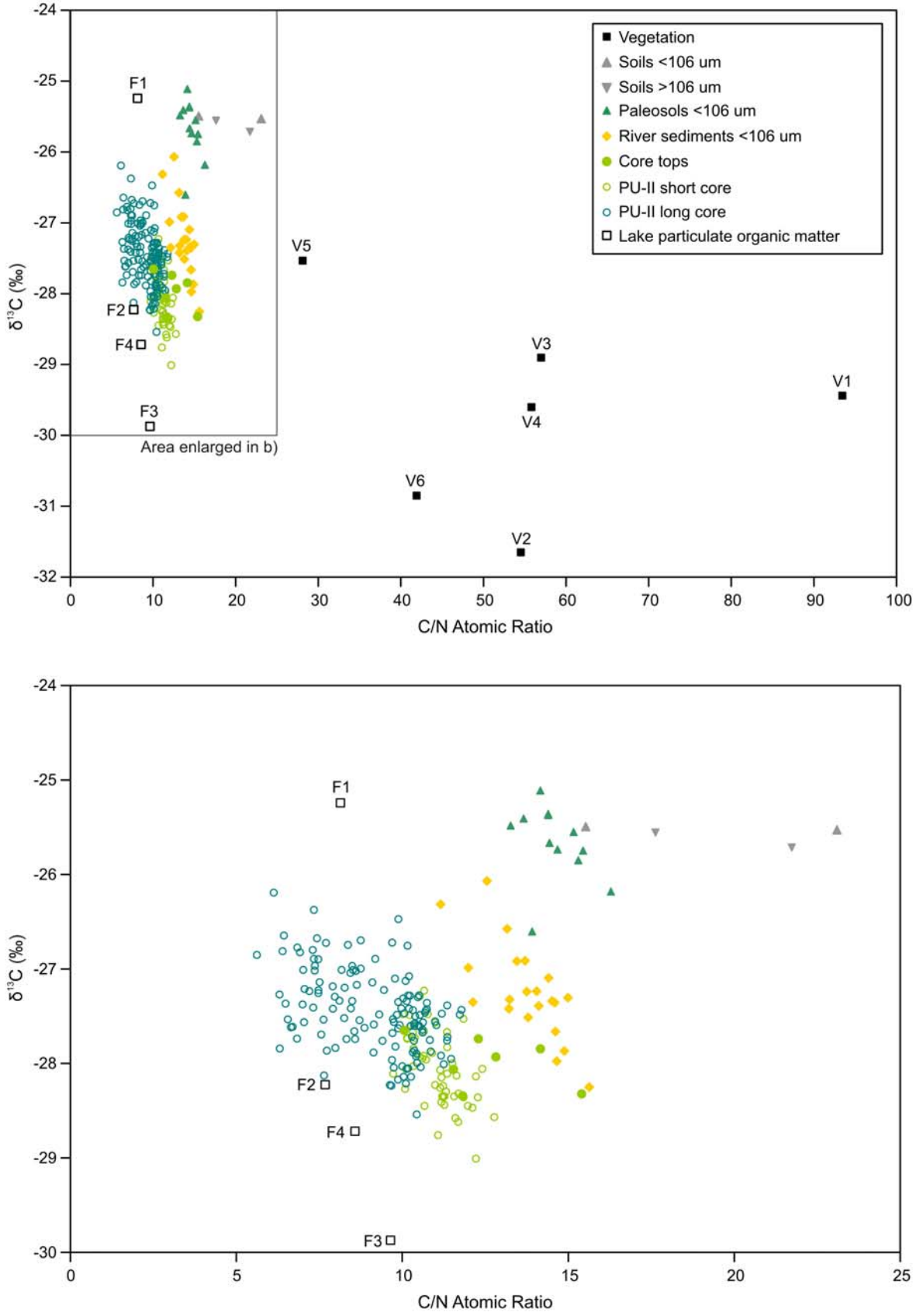

1121

1122 Bertrand et al – Figure 3

1123

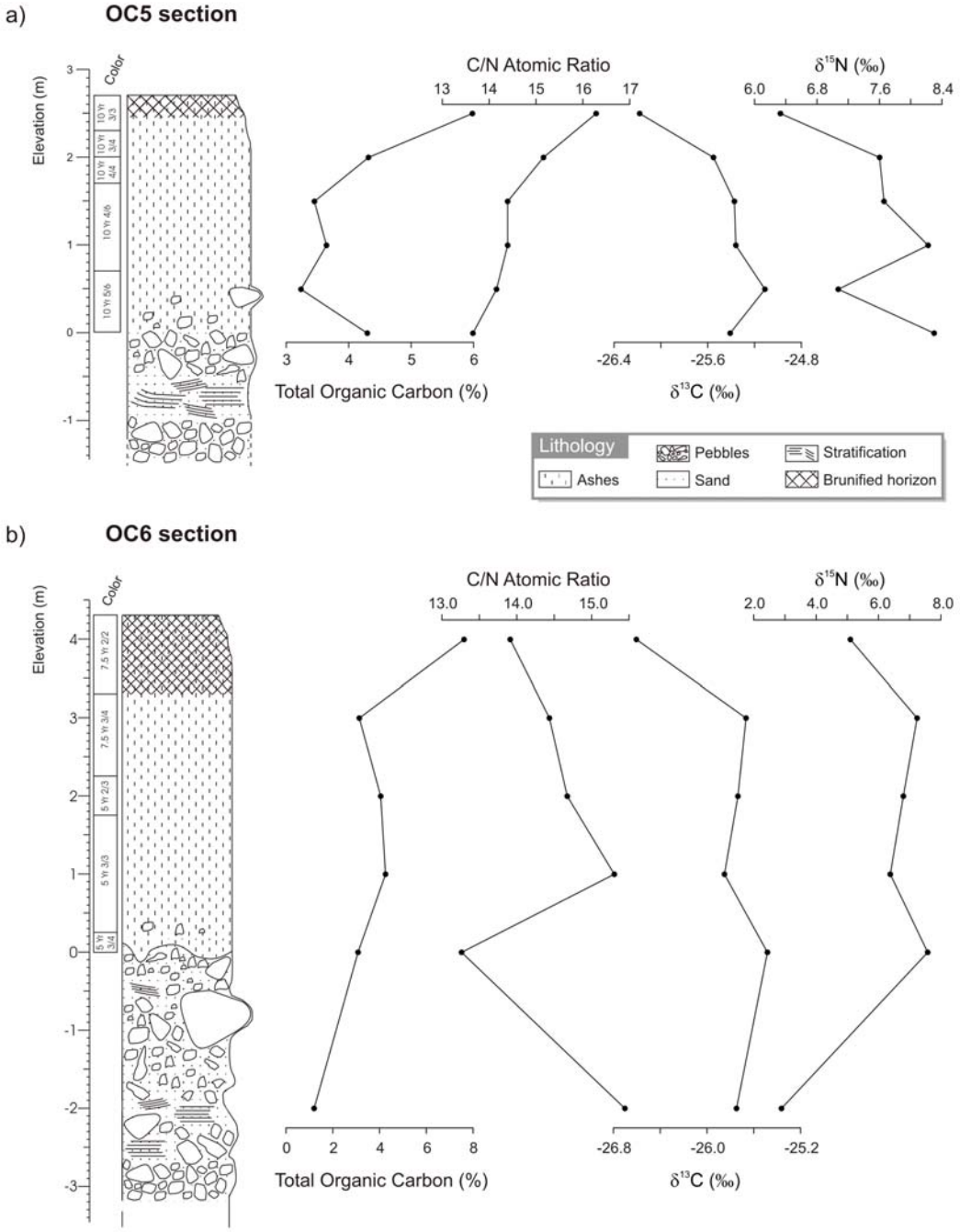

1124

1125 Bertrand et al – Figure 4

1126

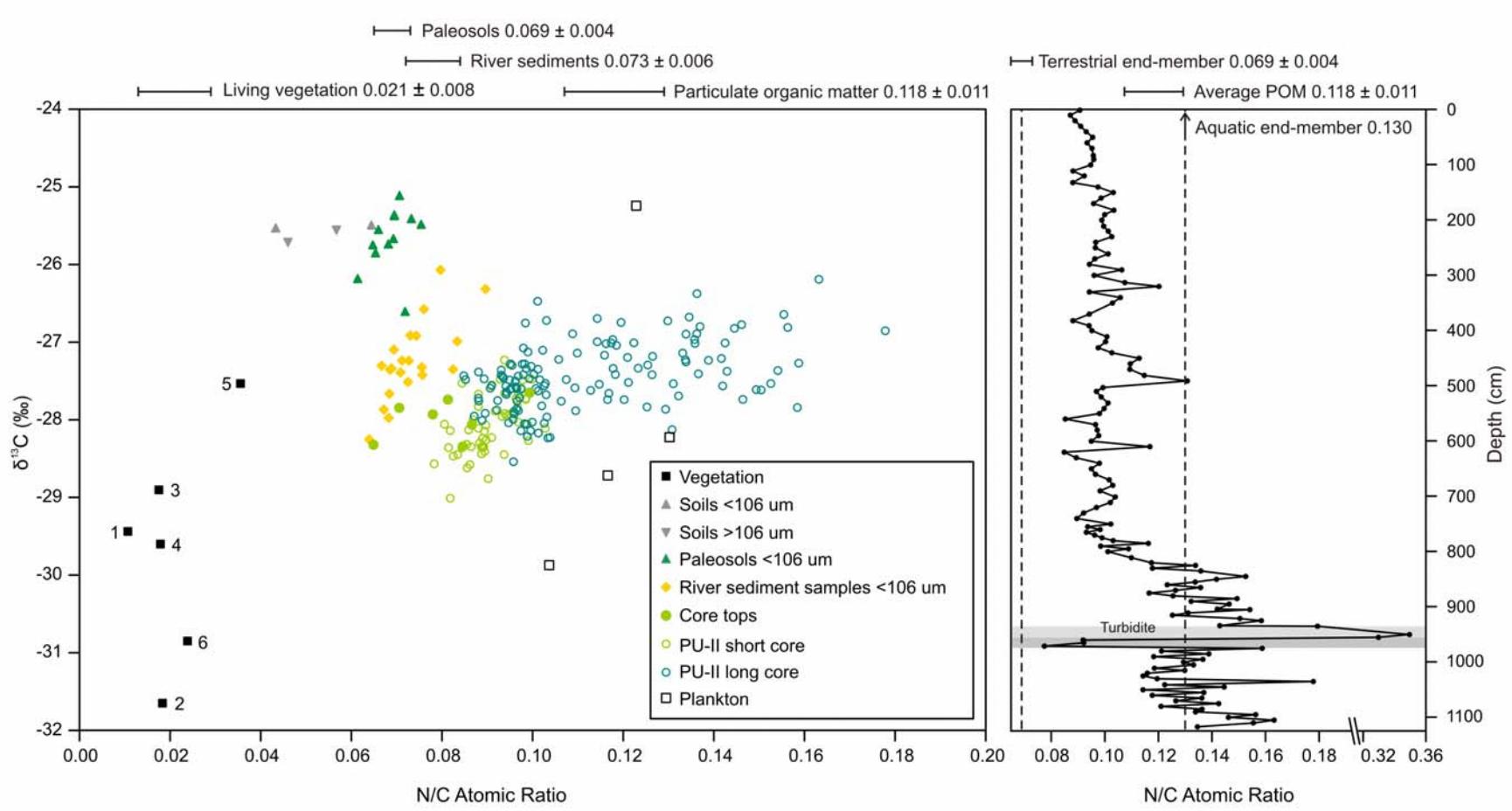

1127

1128 Bertrand et al – Figure 5

1129

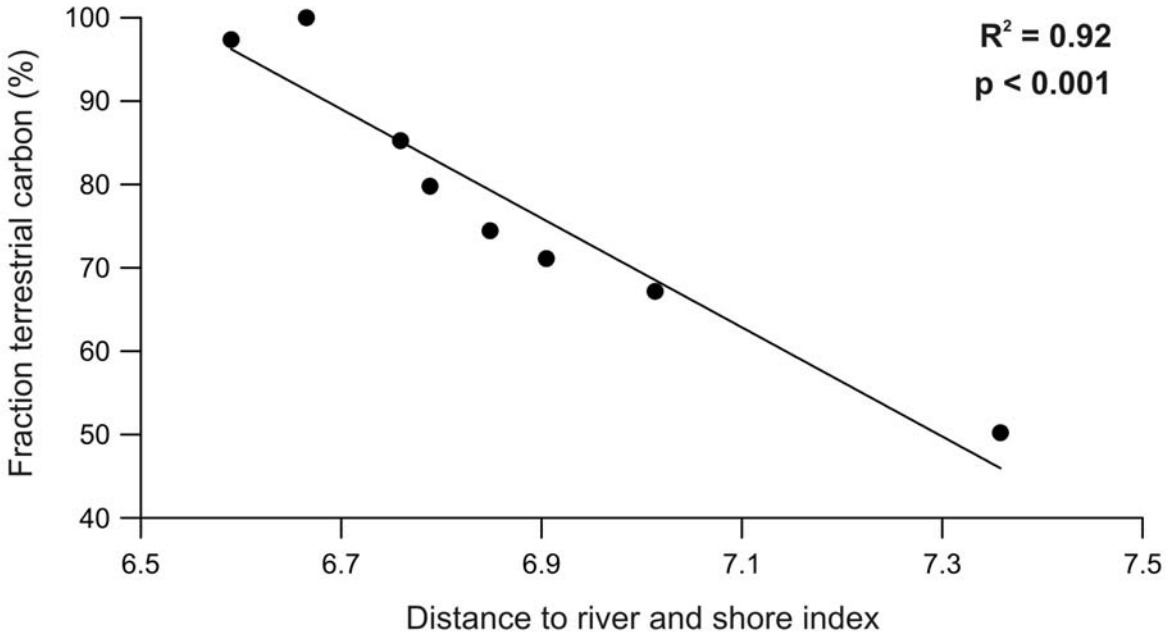

1130

1131 Bertrand et al – Figure 6

1132

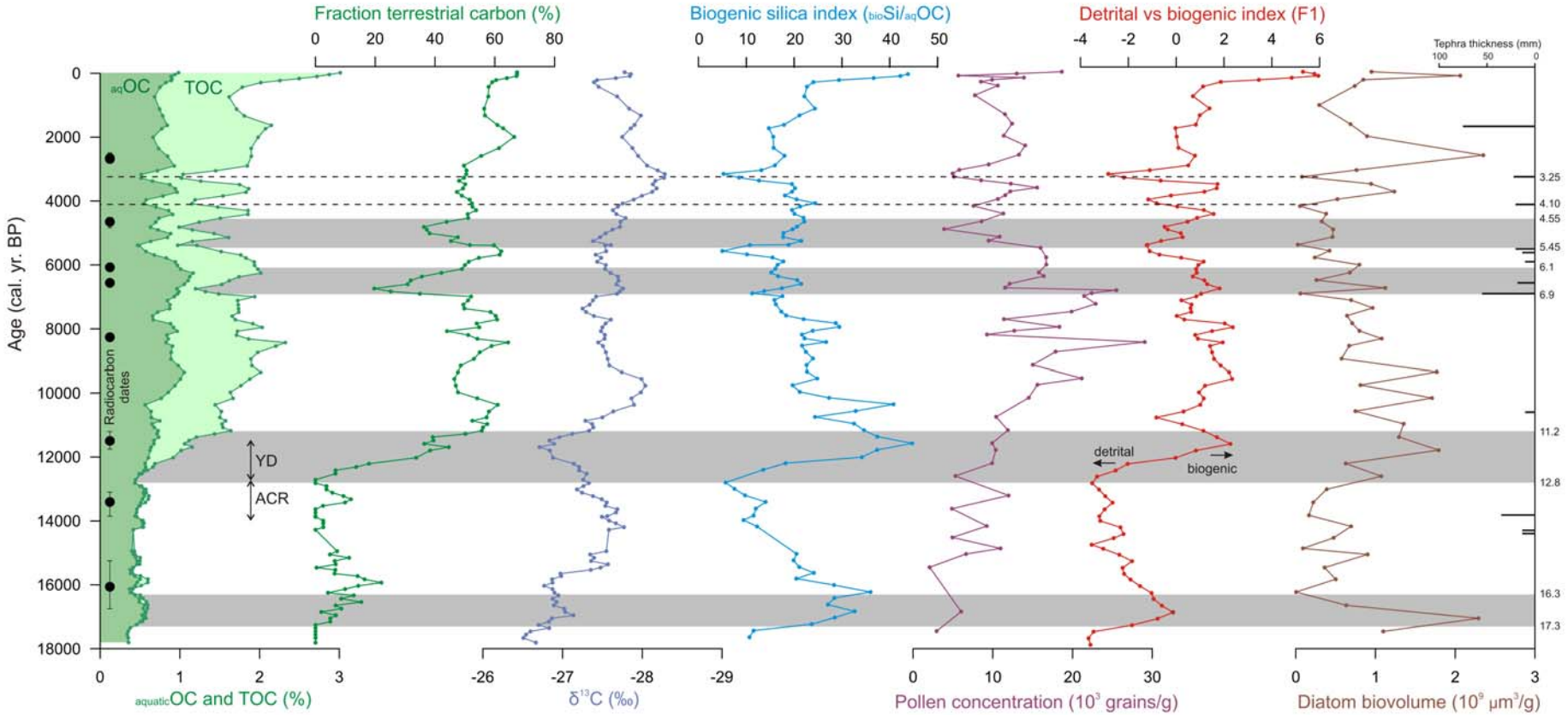

1133

1134 Bertrand et al – Figure 7

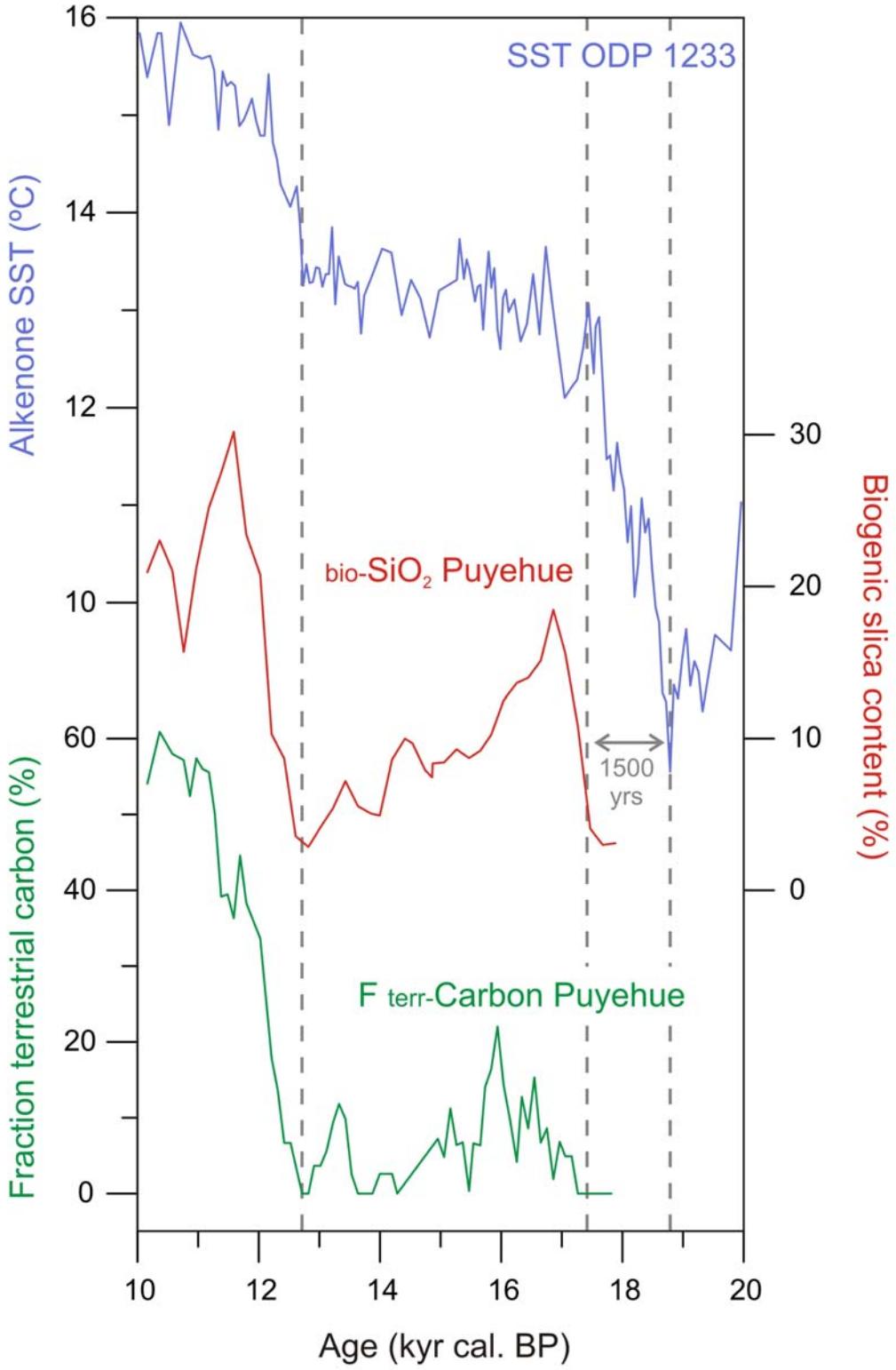

Bertrand et al – Figure 8